

1 **Seismic and borehole-based mapping of the late Carboniferous succession in**
2 **the Canonbie Coalfield, SW Scotland: evidence for a ‘broken’ Variscan**
3 **foreland?**

4 Louis Howell^{1*}, Bernard Besly¹, Surika Sooriyathasan¹, Stuart Egan¹, Graham Leslie²

5 ¹School of Geography, Geology and the Environment, Keele University, Staffordshire, ST5 5BG, UK

6 ²British Geological Survey, The Lyell Centre, Edinburgh, Currie EH14 4BA, UK

7 *l.p.howell@keele.ac.uk

8 **Abstract**

9 Local seismic and borehole-based mapping of the Carboniferous Pennine Coal Measures and
10 Warwickshire Group successions in the Canonbie Coalfield (SW Scotland) provides evidence of
11 repeated episodes of positive inversion, syn-depositional folding and unconformities. A Duckmantian
12 (Westphalian B) episode of NE-SW transpression is recognised, based on onlapping seismic reflector
13 geometries against NE-trending positive inversion structures and contemporaneous NNE-trending
14 syn-depositional growth folding. The basin history thus revealed at Canonbie is at variance with
15 generally accepted models in neighbouring northern England that imply subsidence was due to post-
16 rift thermal subsidence during late Carboniferous times. A late Westphalian-Stephanian
17 unconformity recognised within the Warwickshire Group succession signifies NW-SE, c. 10 % local
18 basin shortening during a time of major shortening in the late Carboniferous Variscan foreland,
19 contradicting suggestions that maximum Variscan shortening had negligible impact on Carboniferous
20 basins in northern Britain. Local inversion structures appear to have strongly influenced local late
21 Westphalian-Stephanian depocentres. In this respect, the Variscan foreland at Canonbie may have
22 resembled a ‘broken’ foreland system. Variations in crustal rheology, fault strength and orientation,

23 and mid-crustal detachments are suggested to have played important roles in determining strain
24 localisation and the nature of Westphalian-Stephanian depocentres in the Canonbie Coalfield.

25 **1. Introduction**

26 One of UK coal mining's legacies is the vast quantity of subsurface data that we inherit.
27 These data record an important chapter of the Earth's history, the amalgamation of Pangaea, and
28 have the potential to be widely repurposed as the UK seeks to decarbonise and fulfil its energy
29 needs through more sustainable resources (Watson *et al.*, 2019). We present a study based on
30 subsurface (seismic and borehole) data from the Canonbie Coalfield in SW Scotland (see Fig. 1 for
31 location). These coal-bearing strata were deposited in the northern British part of an expansive late
32 Carboniferous Variscan foreland basin system, the complex characteristics of which have been
33 debated for decades (Leeder, 1982; Coward, 1993; Ziegler, 1993; Woodcock and Rickards, 2003;
34 Underhill *et al.*, 2008). In both modern and ancient foreland systems, syn-kinematic sedimentary
35 sequences can indirectly reveal the nature of the various tectonic episodes that influenced the basin
36 and its regional setting. In ancient foreland systems, these sequences are often absent due to later
37 uplift and denudation. In contrast, a near complete record of the late Carboniferous syn-kinematic
38 megasequence (e.g. Besly *et al.*, 1993; Peace and Besly, 1997) is locally preserved at the Canonbie
39 Coalfield (Chadwick *et al.*, 1995; Waters *et al.*, 2011; Jones *et al.*, 2011).

40 Using archived seismic and borehole datasets curated by the UK Onshore Geophysical
41 Library (UKOGL) and the British Geological Survey (BGS), we investigate the characteristics of the
42 preserved late Carboniferous syn-kinematic sedimentary sequence preserved in the Canonbie
43 Coalfield, and the tectonic controls that were exerted upon its depositional and post-depositional
44 deformation. Widely held perceptions of ancient foreland basin systems such as the Variscan
45 foreland, often portray these systems in broadly two-dimensional perspectives on tectonic scales.
46 These systems include a single collision zone adjacent to a region of subsidence occurring primarily
47 along a restricted, laterally migrating flexure-induced foredeep depozone. Deposition also occurs to

48 lesser extents within forebulge and backbulge depozones. A simplistic laterally dissipating
49 compressional stress field is typically derived from a short-lived contractional episode (e.g. DeCelles
50 and Giles, 1996; DeCelles, 2012; Catuneanu, 2019). However, at Canonbie we demonstrate syn-
51 depositional faulting, folding and positive inversion exerted strong controls on early Westphalian
52 (Bashkirian) through to Stephanian (Kasimovian) depocentres. Such behaviour is not just at variance
53 with generally accepted models for late Carboniferous basin development in neighbouring northern
54 and central England therefore, but also with many conceptual models for generic foreland basin
55 systems. Evolution of the Canonbie Coalfield and its regional setting is perhaps more akin to ‘broken’
56 foreland systems such as in the eastern Andean retro-arc foreland of Patagonia where
57 sedimentation is controlled by local tectonism (e.g. Strecker *et al.*, 2011; Bilmes *et al.*, 2013). We
58 attempt to reconcile competing tectonic models for the northern British part of the Variscan
59 foreland and demonstrate the importance of inherited crustal structures, the relative susceptibilities
60 of these structures to reactivation and the influence of an evolving stress field on the characteristics
61 of the syn-kinematic sedimentary sequence preserved at Canonbie.

62 **2. Regional geological setting**

63 In northern Britain, there are two models for late Carboniferous tectonic evolution. The first
64 focuses upon inversion tectonics following early Carboniferous rifting and post-rifting, relating to a
65 dissipating stress field derived from the Variscan collision zone of central-southern Europe (Leeder,
66 1982; Corfield *et al.*, 1996). The Variscan orogen formed in southern-central Europe in response to
67 approximately northward accretion of early Palaeozoic island arcs and continental fragments and
68 later Gondwanan-derived elements onto Laurussia during the prolonged late Palaeozoic assembly of
69 Pangaea (Warr, 2012; Murphy *et al.*, 2016; Shaw and Johnston, 2016; Edel *et al.*, 2018). The orogen
70 reached its maximum intensity during the late Carboniferous, culminating with the closure of the
71 Palaeotethys Ocean and the formation of the Cantabrian and central Iberian oroclines (c. 310-295
72 Ma) (Murphy *et al.*, 2016). The northern margin of this belt can be traced approximately east-west

73 across southern England where it separates the late Carboniferous foreland basin of southern Wales
74 (Burgess and Gayer, 2000) from the low-grade metamorphic external Variscan thrust belt and early
75 Carboniferous foredeep (Murphy *et al.*, 2016). Within the British Variscan foreland region, the
76 magnitude of dominantly oblique contemporaneous thrust and fold inversion structures generally
77 increases towards the Variscan Front (Fraser and Gawthorpe, 1990; Corfield *et al.*, 1996; Woodcock
78 and Rickards, 2003; Warr, 2012). This style of deformation is analogous to modern day shortening
79 exerted between orogenic collision zones and adjacent foreland regions (Copley *et al.*, 2011;
80 Assumpcao, 1992), such as with the Himalayas and northern India (Powers *et al.*, 1998).

81 However, a tectonic model that revolves solely around northward-vergent Variscan
82 compressional stresses does not readily incorporate parallel to oblique late Carboniferous fold and
83 thrust structures such as those that characterise both the Canonbie Coalfield and the northern
84 British Variscan foreland (Fig. 1). Copley and Woodcock (2016) calculate that such discontinuities
85 must have been significantly weaker (with an effective co-efficient of friction at least less than 30 %
86 lower) than intact country rock for them to have reactivated during Variscan compression rather
87 than new faults initiate. Coward's (1993) alternative tectonic model for the Variscan foreland
88 highlights the influences of dextral strike-slip movement along pre-existing and long-lived NW-SE
89 trending thick-skinned faults; wrench movement along structures such as the Southern Upland Fault
90 Zone in southern Scotland accommodated westwards reinsertion of Baltica between North America
91 and central-southern Europe. Reinsertion is believed to have been a response to the
92 contemporaneous, but distal, Uralian Orogeny. The Uralian Orogeny formed as the result of
93 accretion of the Siberian and Kazakh plates against Baltica's eastern (Laurussian) margin and the
94 closure of the Ural Ocean; orogeny began during the late Carboniferous and continued into the early
95 Jurassic (Bea *et al.*, 2002; Brown *et al.*, 2006).

96 **3. Seismo-stratigraphic analysis of the Canonbie Coalfield**

97 **3.1 Datasets**

98 A number of datasets have been utilised in the study of the late Carboniferous succession at
99 Canonbie (Fig. 2). These include 12 UK Oil and Gas Authority and 7 UK Coal Authority onshore digital
100 2D seismic reflection profiles, originally acquired by Edinburgh Oil & Gas Ltd. and by the British Coal
101 Corporation respectively. Seismic surveys for coal exploration are typically shot at higher frequencies
102 (<125 Hz) and with lower depths of penetration than surveys for oil and gas exploration (20-80 Hz;
103 Gochioco, 1990). Seismic reflection profiles shot for coal exploration therefore enable detailed
104 mapping of onlapping and truncated seismic reflection geometries within sedimentary units at
105 shallow depths, helping to constrain the timing of various deformation events. Note that the seismic
106 reference datum from which the seismic reflection profiles are plotted for British Coal exploration
107 surveys often varies from the sea level datum typically used for oil and gas surveys. Where the coal
108 exploration datum was flat but shot above sea level, the reflection profile was shifted vertically in
109 two-way travel time, assuming a constant near surface velocity of 2400 ms⁻¹. Where the reference
110 datum was sloping, the reflection profile was not used for mapping in this study. These data are
111 supported by 19 borehole penetrations, all of which provide stratigraphic constraints and some of
112 which are associated with petrophysical (mainly gamma ray and acoustic) data and time-depth
113 calibration data. These boreholes were drilled between 1854 and 2008 for coal, oil and gas and
114 coalbed methane exploration purposes (Picken, 1988; Creedy, 1991; Chadwick *et al.*, 1995). The
115 quality of data associated with each borehole varies accordingly. We encourage readers to follow
116 web links to uninterpreted versions of our seismic lines, which can be found in the figure captions.

117 *3.2 Stratigraphy*

118 In accordance with previously published UK literature and industrial reports, the traditional
119 NW European Carboniferous chronostratigraphic subdivisions have been adopted (Waters *et al.*,
120 2011; Davydov, 2004); these subdivisions and the current international subdivisions are correlated in
121 Figure 3.

122 The Canonbie Coalfield is situated on the Scottish-English border within the northern Solway
123 Carboniferous Basin. The coalfield is one of few places in the UK that preserves a near complete
124 Westphalian stratigraphic record (Fig. 3). The Canonbie stratigraphic succession consists of <300 m
125 of Langsettian-Duckmantian (Westphalian) Pennine Lower and Middle Coal Measures Formations
126 (*herein*: PLCM and PMCM). Ordinarily, in north-western Europe, the base of this succession is
127 defined by the *Subcrenatum* Marine Band (Waters *et al.*, 2011). This unit is absent at Canonbie, and
128 across the entirety of the Midland Valley of Scotland (Cameron and Stephenson, 1985; Dean *et al.*,
129 2011) such that the Pennine Coal Measures Group (PCM) rests disconformably upon the underlying
130 Namurian succession. The PCM succession is correlative across both the coalfield and NW Europe
131 based on frequent stratigraphically defined coal seams and marine bands. The Pennine Upper Coal
132 Measures Formation (PUCM) is poorly documented in historical accounts of the Canonbie Coalfield
133 and contains only limited amounts of coal-bearing strata that provide stratigraphic control. Similarly-
134 aged stratigraphy can be recognised further afield in southern Scotland as well as in Cumbria,
135 courtesy of inter-bedded *Spirorbis*-bearing limestone beds (Mykura, 1967).

136 Overall upwards-coarsening and primarily 'red-bed' Warwickshire Group strata, conformably
137 overlie PCM strata at Canonbie (Fig. 3) (Jones *et al.*, 2011). Given the poor likeness of the
138 Warwickshire Group strata at Canonbie with the Warwickshire Group Whitehaven Sandstone
139 Formation of West Cumbria, and the paucity of stratigraphically correlative strata from both
140 locations, three locally-defined formations are used to describe the succession at Canonbie (Jones *et*
141 *al.*, 2011). These are the Eskbank Wood, Canonbie Bridge Sandstone and Becklees Sandstone
142 formations. Only strata of the *Tenuis* Chronozone (lower Westphalian D) have been proved within
143 the lowermost mudstone dominated Eskbank Wood Formation (Jones *et al.* 2011). No
144 biostratigraphically-defined age constraints are given for the remainder of the Warwickshire Group.
145 However, the Canonbie Bridge Formation shares petrographic characteristics with the Halesowen
146 Formation of the English Midlands and is believed to be of predominantly Asturian (Westphalian D)
147 age also (Jones *et al.*, 2011; Morton *et al.*, 2015). A chronostratigraphic correlation of the late

148 Westphalian-Stephanian succession preserved at Canonbie across southern Scotland, northern
149 England and central England is included in figure 3.

150 *3.3 Seismic horizons and time-depth conversion*

151 Several latest Devonian to Permian-aged seismo-stratigraphic horizons were mapped in two-
152 way travel time. The most consistent mappable surface is the base Permian angular unconformity
153 against which Carboniferous reflectors truncate upwards. The Westphalian-Stephanian succession is
154 characterised by strong, semi-continuous seismic reflectors due to the presence of thick inter-
155 bedded channel sands (Jones *et al.*, 2011) and low-density coals (Picken, 1988). Based on similar
156 studies within the region (Kimbell *et al.*, 1989; Chadwick *et al.*, 1995), a single strong, positive,
157 continuous reflector is believed to mark the Great Limestone Member (Alston Formation, Yoredale
158 Group) at the base of the Canonbie Namurian succession. Below this unit, similar inter-bedded
159 limestone-derived reflectors characterise the Visean succession of the Tyne Limestone Formation
160 (also Yoredale Group). The top Caledonian (lower Palaeozoic) basement horizon is interpreted as
161 being represented by a series of strong positive continuous reflectors that are believed to represent
162 subsurface equivalents of the Birrenswark Volcanic Formation (Inverclyde Group) (*cf.* Kimbell *et al.*,
163 1989).

164 Bulk sonic velocities for the Permian succession (2900 ms^{-1}), the Westphalian-Stephanian
165 succession (3600 ms^{-1}) and the latest Devonian-Namurian succession (4500 ms^{-1}) were used to
166 construct a simple velocity model. These values were derived from sonic velocity log data for the
167 Easton, Timpanheck and Becklees boreholes. A seismic velocity of 5000 ms^{-1} was used for the
168 basement (*cf.* Evans, 1994). The velocity model was used to convert the seismic surveys from time to
169 depth domain. Although uncertainty surrounding the time-depth conversion process is
170 acknowledged, the velocity model is deemed adequate for the purposes of the structural
171 interpretation reported in this study. Stratigraphic data derived from borehole reports was used to
172 better constrain structural interpretations of the depth converted seismic survey.

173 **4. Structure of the Canonbie Coalfield**

174 To understand the late Carboniferous kinematic evolution of the Canonbie Coalfield better,
175 we present an integrated interpretation of the depth-converted seismic dataset, borehole data and
176 outcropping geology. Several key structures have been identified as a result of that analysis (Fig. 5a).
177 These include: 1) the NE-SW trending Bewcastle anticline and Hilltop Fault; 2) the NNE-SSW trending
178 Solway syncline; 3) the NE-SW trending Gilnockie Fault; 4) ENE-WSW and E-W trending normal faults
179 such as the Archerbeck, Rowanburn, Woodhouselees and Glenzierfoot Faults, and; 5) (N)NW-(S)SE
180 trending strike-slip faults such as those exposed at surface laterally offsetting the coalfield's Permian
181 cover. We describe the Westphalian-Stephanian succession through a series of time-slices, focussing
182 upon how this succession was influenced by the combined effects of these key structures during its
183 deposition.

184 *4.1 Namurian and Pennine Lower Coal Measures (PLCM)*

185 Based on isochore thickness maps (Fig. 5b-d), and unlike the general case across the Midland
186 Valley of Scotland (Ritchie *et al.*, 2003; Underhill *et al.*, 2008), Namurian and PLCM stratigraphy at
187 Canonbie shows little evidence of varying significantly in thickness across the coalfield (Fig. 5b);
188 although, this is in contrast with the southern part of the Solway Basin where Chadwick *et al.* (1995)
189 observed mild thickening within the southern trough of the Solway Syncline and Akhurst *et al.* (1997)
190 records a localised late Namurian angular unconformity. The local PCM subcrop is bound to the
191 northwest by the Gilnockie Fault and to the southwest by the Hilltop Fault that both dip towards the
192 southeast and display net normal and reverse displacement respectively. From seismic data, Picken
193 (1988) interpreted a known local basal Westphalian break in deposition (represented by the absence
194 of the *Subcrenatum* marine band) as a low-angle overstepping unconformity that resulted from syn-
195 depositional anticlinal growth along a c. N-S compressional axis (e.g. Fig. 10 in Picken, 1988). The
196 originally observed outcropping example of this unconformity was argued to represent low-angle
197 unconformable onlap and overstep (Lumsden *et al.*, 1967) but has recently been reinterpreted as,

198 instead, representing a localized sedimentary feature, resulting from multiple phases of river
199 channel-bank collapse (Jones and Holliday, 2016). After careful re-examination of this seismic
200 dataset however, we now interpret the PLCM onlap surface of Picken (1988) as actually representing
201 the Gilnockie Fault, along a 2D seismic profile parallel to the fault, which offsets late Carboniferous
202 strata as well as the strata below it (Fig. 6). The absence of basal Westphalian stratigraphy at
203 Canonbie, we believe, represents a parallel disconformity.

204 *4.2 Pennine Middle and Upper Coal Measures (PMCM and PUCM)*

205 Variations in the thickness of PMCM and PUCM stratigraphy (Figs. 5c, d) suggest that the
206 NNE-SSW trending Solway Syncline acted as a significant depocentre for Duckmantian and younger
207 Westphalian stratigraphy (also see Fig. 7). Throughout the coalfield, these units also thicken
208 gradually towards the Hilltop Fault, within the fault's footwall, but are at their thickest (<700 m)
209 within the Solway Syncline axial zone. This structure forms a broad, slightly asymmetrical syncline in
210 the south-eastern part of the coalfield (Fig. 5a). To the immediate south, a 'minor early
211 Carboniferous high' (Picken, 1988) or local strike-parallel northwards plunge of the Solway syncline
212 marks the southern margin of the Canonbie coalfield. The Solway Syncline continues to the south
213 beyond this 'high', where it meets the northern margin of the early Carboniferous Lake District Block
214 (Chadwick *et al.*, 1995). Whilst the syncline's eastern limb is cross-cut by the Hilltop Fault, its
215 western limb shallows progressively towards the north and west. In the north-western part of the
216 coalfield, a series of bright reflectors within the PMCM can be seen gently onlapping against similarly
217 bright reflectors along the syncline's western limb (Fig. 8, and inset Fig. 8b). Based on borehole
218 stratigraphy, the reflector that most closely resembles the surface of onlap is thought to represent
219 the approximately late Duckmantian (Westphalian B) Archerbeck coal seam (also PMCM) (Fig. 4).

220 Synthetic and antithetic faults that merge with the Gilnockie Fault at 1-2 km depth, spatially
221 correlate with the upper limit of the Solway Syncline's western limb (Fig. 8), onto which the Upper
222 Coal Measures and younger Westphalian stratigraphy thin gently (Fig. 5c, d). The *Cambriense* Marine

223 Band (locally referred to as the *Skelton* Marine Band) that marks the base of the PUCM succession is
224 locally absent in borehole penetrations along the north-western margin of the Canonbie Coalfield
225 (Timpanheck, Bogra and Beckhall; Fig. 2). The underlying stratigraphic units form a series of mild,
226 together <2 km wide, parallel trending anticlines, which are overstepped by younger Westphalian
227 stratigraphy (Fig. 8). These mild folds are together tilted south-eastwards by the coalfield wide
228 Solway syncline. As with the Hilltop Fault, along the south-eastern margin of the coalfield, latest
229 Devonian-Visean units (Inverclyde and Border Groups) within the hangingwall of the Gilnockie Fault
230 thicken gently towards the fault, indicating normal movement at the time of latest Devonian-Visean
231 deposition.

232 Evidence from borehole stratigraphy suggests that minor thickness increases in PMCM and
233 PUCM units towards the ENE-WSW to E-W trending Archerbeck, Rowanburn, Woodhouselees and
234 Glenzierfoot Faults within their hanging walls may be tentatively interpreted based on seismic
235 reflection profiles, although growth of the Solway Syncline appears to have had a greater influence
236 on thickness distribution of Westphalian stratigraphy. These structures all appear to dip steeply
237 towards the south, displacing Carboniferous stratigraphy in a normal sense (Fig. 6). Latest Devonian
238 to early Carboniferous-aged units (Inverclyde and Border Groups) are offset normally by and may be
239 tentatively interpreted as gently thickening towards the Archerbeck, Rowanburn, Woodhouselees
240 and Glenzierfoot Faults within their hanging walls, as they do towards the major parallel fault
241 systems that bound the Solway Basin to the south (Chadwick *et al.*, 1995).

242 4.3 Warwickshire Group

243 Although much of the subcropping Warwickshire Group succession has been partly eroded
244 prior to Permian deposition, thus limiting further use of isochore thickness maps, reflector
245 geometries observed within the Canonbie Bridge and Becklees Sandstone Formations in the Solway
246 syncline trough suggest that the nature of this depocentre was altered during deposition of the
247 Becklees Sandstone Formation. In higher resolution coal exploration seismic reflection profiles, a

248 thick succession (< 200 m) of Becklees Sandstone Formation can be observed showing angular onlap
249 against the Canonbie Bridge Sandstone Formation stratigraphy within the Solway syncline's western
250 limb (Fig. 9). In addition, reflectors belonging to the Canonbie Bridge Sandstone Formation within
251 the syncline's western limb are slightly truncated against the surface of onlap (marked u/c 3; Fig.
252 9b). This surface of onlap is interpreted as an angular, partially erosional, unconformity. An
253 additional unconformable horizon can be observed from the seismic data and down cuts into
254 younger Becklees Sandstone stratigraphy within the Solway syncline, truncating underlying
255 reflectors (u/c 4; Fig. 9b). Given that the Becklees Sandstone Formation has been interpreted as
256 having been deposited in a fluvial environment (Jones *et al.*, 2011) and given the broad U-shape
257 geometry of the unconformity, this feature is interpreted as representing an erosive and, most likely,
258 confined fluvial channel set (*cf.* Ramos *et al.*, 2002). Above angular unconformity u/c 3 (Fig. 9b), the
259 axis of the Solway syncline appears to have migrated south-eastwards towards the Hilltop Fault.
260 Given the discordance between reflectors within the Canonbie Bridge and Becklees Sandstone
261 Formations in the syncline's western limb (Fig. 9a), this eastwards migration of the Solway syncline
262 depocentre is most likely associated with a steepening of this western limb. In addition, and along
263 the syncline's north-western limb, the entirety of the Carboniferous succession forms a high
264 amplitude (<1 km) anticline with a shorter and shallowly dipping north-western limb (Fig. 9a). This
265 anticline correlates spatially with the Gilnockie Fault, which dips more shallowly, at least locally,
266 within the uppermost 800 m of the subsurface. The onlapping reflector geometries described here
267 within the Warwickshire Group of the Solway syncline (Fig. 9a), constrain the timing of the formation
268 of this anticline to to the earliest deposition of the Becklees Sandstone Formation (*cf.* Fig. 3) (Jones
269 *et al.*, 2011).

270 The NNE-trending Bewcastle anticline occurs within the hanging wall block of the parallel
271 Hilltop Fault. Unlike the comparatively minor anticlines along the north-western margin of the
272 coalfield, there are no timing constraints for the formation of this anticline but it is assumed that

273 they formed at similar times. The Hilltop Fault tips out within the Solway Basin around the southern
274 margin of the coalfield (Chadwick *et al.*, 1995).

275 4.4 Stephanian-early Permian

276 Later Stephanian to early Permian deposits are absent from the Canonbie Coalfield, as is
277 generally the case in the rest of north-western Europe (see Besly and Cleal, *in press*). Both Permian
278 strata and older Carboniferous strata are offset normally by one of the steeper synthetic faults to
279 the Gilnockie Fault as well as ENE- to east-trending faults (Figs. 6, 8). Older Westphalian strata are
280 offset by a greater magnitude along this structure than Permian strata, suggesting that an episode of
281 normal faulting preceded Permian deposition. At least two (N)NW-(S)SE trending faults cut, with
282 apparent dextral offset, the Gilnockie Fault as well as the Permian-aged cover by <500 m along the
283 western margin of the coalfield (Fig. 5a); this pattern is consistent all across the Northumberland-
284 Solway Basin (de Paola *et al.*, 2005). This group of structures is difficult to identify within seismic
285 reflection profiles, suggesting that their vertical displacement is minimal. A strong degree of
286 uncertainty surrounding the timing of these structures is acknowledged.

287 5. Tectonic controls on the late Carboniferous evolution of the Canonbie 288 Coalfield

289 We believe that the fragmented late Carboniferous kinematic evolution of the Canonbie
290 Coalfield can be constrained by at least three episodes of deformation (Fig. 10). These three
291 episodes of deformation can be represented by unconformities described in the PMCM and the
292 Warwickshire Group respectively (Figs. 8 and 9) as well as later normal fault movement prior to
293 deposition of the basal Permian succession at Canonbie (Fig. 6).

294 5.1 Pennine Coal Measures (PCM) unconformity

295 Based on isochore thickness distributions for PMCM and PUCM and asymmetric, low-
296 amplitude folding correlating spatially with the Gilnockie Fault, the local PMCM unconformity is

297 interpreted to indicate significant syndepositional tectonism. Although folding of the entire
298 Carboniferous succession beneath the base Permian unconformity has ultimately distorted the
299 nature of the PMCM unconformity, 2D palinspastic cross-section restoration of a NE-SW section
300 through the Canonbie Coalfield and Gilnockie Fault reveals that low amplitude folding occurred at
301 the same time as this unconformity (Fig. 10c), resulting in 1.4 % along length shortening. Along
302 strike, the steeper sided limbs of asymmetric, low-amplitude folds correlate laterally with the
303 steeply dipping synthetic and antithetic normal faults of the Gilnockie Fault (Fig. 8), although there is
304 interference between adjacent folds. Previous studies of inverted basins suggest that similar
305 asymmetric, low-amplitude folding can be indicative of 'mild' positive fault inversion (*sensu* Song,
306 1997) - where the 'null point' or the point along an inverted fault's length at which there is zero net
307 displacement (*sensu* Williams *et al.*, 1989) remains at the fault's upmost tip (*cf.* Butler, 1998; Jackson
308 *et al.*, 2013). Mild inversion structures are strongly dominated by folding due to partial reverse
309 reactivation of a fault along its length, where thrusting does not accommodate a significant amount
310 of shortening (Jackson *et al.*, 2013). Compressional stress at the time of folding is insufficient to
311 prompt full reverse reactivation of these faults. The asymmetrical nature of the local PMCM and
312 PUCM depocentre in the Canonbie Coalfield can be explained by these asymmetric and mild
313 inversion structures (Figs. 5 and 8). Oblique-slip (dextral) movement along similar NE-SW trending
314 structures, such as the Gilnockie and Hilltop Faults, may have contributed to the slightly oblique
315 NNE-SSW trending growth of the Solway syncline with respect to these faults.

316 *5.2 Warwickshire Group unconformity*

317 The Warwickshire Group unconformity appears to represent a more significant
318 rearrangement of the local foreland basin system. Two-dimensional palinspastic restoration of the
319 NW-SE striking cross-section illustrated in figure 9 suggests that the Warwickshire Group
320 unconformity, seen in seismic data along the buried axis of the Solway syncline (Fig. 9), formed
321 because of anticlinal folding due to shallowly dipping basement-involved thrusting along the
322 Gilnockie Fault. This second basin reorganisation episode resulted in at least 10 % shortening (Fig.

323 10b). Unlike prior inversion that occurred during the deposition of the PMCM, shortening occurring
324 during deposition of the younger Warwickshire Group succession appears to have been partly
325 accommodated by the most shallow, comparatively shallowly-dipping part of the Gilnockie Fault (*cf.*
326 Fig. 9a). As this part of the fault does not appear to have accommodated significant extension or
327 shortening prior to this later episode of basin inversion, this part of the fault may have originated as
328 a footwall short-cut (*cf.* Hayward and Graham, 1989). The Warwickshire Group unconformity
329 represents a significant rearrangement in the nature of the local Solway Syncline depocentre (Fig.
330 9a). Folding and thrusting appears to have caused a steepening of the syncline's north-western limb,
331 and perhaps in doing so, confined the local longitudinal fluvial system causing it to become more
332 erosive (*cf.* Ramos *et al.*, 2002; Suriano *et al.*, 2015). Major reverse movement along the Hilltop Fault
333 at this time and the resulting uplift of the hanging wall may have constituted a minor lithospheric
334 load along the coalfield's south-western margin (*cf.* Karner and Watts, 1983). This would have
335 perhaps prompted additional localised flexure-induced accommodation and restricted uplift of the
336 Solway syncline's eastern limb and supplied the coalfield with an additional source of local clastic
337 detritus (*cf.* Jones *et al.*, 2011). The minor Carboniferous high, that marks the southern limit of the
338 coalfield (Picken, 1988; Chadwick *et al.*, 1995), may be attributed to the Hilltop Fault pinching out
339 laterally at a similar latitude if the depocentre immediately to the north (the coalfield) were partly
340 attributed to local flexure-induced subsidence.

341 *5.3 Basal Permian unconformity and latest Westphalian-early Permian relaxation*

342 The post-Westphalian kinematic evolution of the coalfield, prior to deposition of the
343 Permian succession appears to be represented by a 'relaxation' in compressional stresses (*cf.*
344 Dempsey, 2016). Normal offset occurs primarily along pre-existing E-W orientated faults, perhaps
345 indicating dextral transtension (*cf.* Coward, 1993; Monaghan and Pringle, 2004; De Paola *et al.*, 2005;
346 Pharaoh *et al.*, 2019) but also along the Gilnockie Fault (Fig. 8). The basal Permian angular
347 unconformity cuts stratigraphy below it, perhaps suggesting further uplift prior to Permian

348 deposition following the late Westphalian-Stephanian (*cf.* Underhill and Brodie, 1993), although this
349 uplift event appears not to have been accommodated by fault movement.

350 **6. A comparison with the modern ‘broken’ Northern Patagonian foreland** 351 **basin system**

352 We suggest that syn-depositional faulting, folding and positive inversion influenced late
353 Carboniferous depocentres in the Canonbie Coalfield. In this respect, the coalfield provides evidence
354 that suggests that northern Britain during late Carboniferous times was one of many basins that did
355 not fit perfectly within a traditional post-rift tectonostratigraphic framework (e.g. McKenzie, 1978).
356 Instead, the coalfield, which was situated in the distal Variscan foreland system, evokes similarities
357 between the northern British part of the Variscan foreland basin system and the ‘broken’ foreland
358 basin systems (e.g. Bilmes *et al.*, 2013). Whereas traditional foreland basin system models imply that
359 regional geodynamic processes cause expansive and largely uninterrupted basin systems (DeCelles
360 and Giles, 1996), in ‘broken’ foreland systems palaeodrainage, sediment routing and subsidence
361 trends are frequently disrupted by uplifted intra-foreland basin blocks (Strecker *et al.*, 2011). The
362 archetypal example of this type of basin is the modern ‘broken’ Northern Patagonian foreland in
363 Argentina, which is adjacent to the Andean Mountains (Bilmes *et al.*, 2013; Gianni *et al.*, 2015; Lopez
364 *et al.*, 2019; Bucher *et al.*, 2019) (Figs. 11a and c). Here, several narrow Quaternary-aged
365 depocentres still exist oblique to the predominant collision zone and some up to 1000 km away from
366 the oceanic subduction zone (Gianni *et al.*, 2015). These depocentres are defined by comparatively
367 uplifted intra-foreland basement blocks that have been reactivated contemporaneously with
368 Andean collision after having initially formed as earlier Mesozoic rift basins (Bilmes *et al.*, 2013) (Fig.
369 11c). The (Neogene) syn-kinematic sedimentary sequence is characterised by stratigraphically
370 frequent angular unconformities, and evidence of complex palaeodrainage systems and localised
371 sediment routing (Lopez *et al.*, 2019).

372 As with several of the smaller depocentres that together constitute the 'broken' Northern
373 Patagonian foreland, the late Carboniferous Solway Syncline depocentre appears to have been
374 restricted by the uplift of the Bewcastle Anticline and the limbs of the Solway Syncline from as early
375 as Duckmantian (Westphalian B) times (Fig. 10). The PUCM and Warwickshire Group sediments
376 deposited thereafter are characterised by stratigraphically frequent angular unconformities (*cf.*
377 Lopez *et al.*, 2019). The work of Jones *et al.* (2011), in particular, highlights complex sediment routing
378 and palaeodrainage systems during late Carboniferous times around the Canonbie area. Given the
379 general uncertainty surrounding the youngest Carboniferous sediments of the British Isles (e.g.
380 Besly, 2019), rapid lateral subsidence variations implied by unit thickness variations (Fig. 3) and
381 similarly complex sediment routing and palaeodrainage relationships (Jones *et al.*, 2011), a
382 framework based on the 'broken' Northern Patagonian foreland has the potential to be expanded
383 across the late Carboniferous Variscan foreland basin system (Figs. 11b and d). Further work with
384 similar datasets across the British Variscan foreland, studying the nature of local unconformities and
385 thickness trends within the late Carboniferous succession is however, undoubtedly required before
386 previous assumptions regarding the British Isles at this time can be re-assessed.

387 **7. Discussion**

388 *7.1 Regional tectonic implications*

389 The two intra-Carboniferous unconformities observed in the Canonbie Coalfield
390 approximately correlate with long-recognised angular unconformities in the English Midlands. The
391 earliest PMCM unconformity at Canonbie equates very approximately with the Symon unconformity,
392 a diachronous and generally poorly understood unconformity (or unconformities) that locally
393 separates the Etruria Formation from the onlapping and overstepping Halesowen Formation in the
394 coalfields of Shropshire, South Staffordshire and Warwickshire (Clarke, 1901; Besly and Cleal, 1997;
395 Butler, 2019) (Fig. 3). Poole (1988) also makes this comparison in a comment on Picken's (1988)
396 structural characterisation of the Canonbie Coalfield. Corfield *et al.* (1996) postulate an overall SE-

397 orientated compressional stress field (σ_1) during late Westphalian-Stephanian times. Following the
398 beginning of 'Symon deformation', fluvial red-bed material derived predominantly from the south
399 and south-east began expanding into the basins of the English Midlands (Besly, 1988). Similarly
400 timed phases of deformation are also interpreted by Ritchie *et al.* (2003) within the Scottish Upper
401 Coal Measures Formation based on oil and gas exploration seismic in the eastern part of the Midland
402 Valley of Scotland and implied by an angular unconformity at the base of the Whitehaven Sandstone
403 Formation in West Cumbria (Akhurst *et al.*, 1997).

404 The Warwickshire Group unconformity, which is observed in seismic, crops out along the
405 River Esk, within the study area, and was recognised by Jones *et al.* (2011) who observed polygonal
406 cracks penetrating the underlying Canonbie Bridge Sandstone filled by markedly more poorly-sorted
407 and quartz-rich arenitic Becklees Sandstone Formation, suggesting a prolonged depositional hiatus.
408 Given the great magnitude of shortening and the general absence of pre-Permian compressional
409 deformation accommodated by the Becklees Sandstone Formation in the Canonbie Coalfield, we
410 argue that this unconformity, previously only recognised in outcrop, represents the final major pulse
411 of Variscan inversion in the British Isles (e.g. Peace and Besly, 1997). Tectonostratigraphically
412 equivalent (post-inversion) units in the British Isles may therefore be represented by the Clent
413 Formation of the English Midlands, which unconformably rests on top of the Enville Member (Salop
414 Formation) in South Staffordshire, or the Kennilworth Sandstone Formation, which locally rests
415 unconformably on top of the Tile Hill Mudstone and Salop formations in Oxfordshire (approximately
416 40 km SE) and conformably upon the Tile Hill Mudstone Formation in Warwickshire (Besly and Cleal,
417 1997; Peace and Besly, 1997) (Fig. 3). This may suggest a younger age (Autunian or Gzhelian-
418 Asselian) for the Becklees Sandstone Formation than anticipated prior to this study (*cf.* Besly and
419 Cleal, in press) and that either the polygonal cracks observed by Jones *et al.* (2011) represent a time-
420 gap of up to 8 My or, more likelier, that the Canonbie Bridge Sandstone Formation represents a
421 condensed (200 m thick) time-equivalent unit relative to the far thicker Warwickshire Group
422 successions of central England (>1 km thick) (Fig. 3). Additional sedimentary accommodation in

423 central England may have been a flexural isostatic response to the Variscan Mountains, further to
424 the south. This latest episode of deformation correlates approximately with the c. 310-295 Ma
425 (Murphy *et al.*, 2016) formation of the Iberian and Cantabrian oroclines. Therefore, an alternative
426 more SSW-orientated compressional stress direction could be implied. The Solway syncline has
427 traditionally been associated with Variscan shortening (Chadwick *et al.*, 1995).

428 Attributing late Carboniferous growth of the NNE-SSW trending syncline to either SE or SSW
429 shortening axes (Fig. 5a), creates a series of geometric problems, particularly so in a lower strain
430 setting (*cf.* Copley and Woodcock, 2016). Folding of the NNE-trending Solway Syncline may have
431 alternatively been accommodated by dextral movement along NE-SW trending thick-skinned
432 structures and kinematic strain partitioning (*cf.* De Paola *et al.*, 2005; Leslie *et al.*, 2015). The
433 schematically illustrated two-dimensional strain ellipse for dextral strike-slip movement along NE-
434 SW orientated deep basement faults incorporates simultaneous broadly east-west shortening and
435 broadly north-south extension, echoing early Westphalian growth of the NNE-SSW trending Solway
436 Syncline and mild inversion of the Gilnockie Fault, as well as extension across the broadly east-west
437 trending Rowanburn, Woodhouselees and Glenzierfoot faults (inset Fig. 5a). The structural
438 framework represented by this strain ellipse also accommodates simultaneous strike-slip movement
439 of conjugate faults oblique to the main NE-SW trending faults (e.g. Fig. 6). The localised stress field
440 may have been caused by dextral movement along basement involved faults such as the Gilnockie
441 and Hilltop faults within our study area (Fig. 9), or by distant movement along major thick-skinned
442 faults such as the Southern Upland and Highland Boundary fault systems to the north (Fig. 1). If so,
443 these movements may represent responses to a longer-lived stress regime, derived perhaps from
444 the Uralian Mountains to the east (*cf.* Coward, 1993), which was interrupted sporadically throughout
445 late Carboniferous times by phases of supposed Variscan deformation. Along both the Solway
446 Syncline and across the Midland Valley of Scotland, NNE- to NE-orientated growth folding is proven
447 to have occurred prior to these phases of deformation at Canonbie and throughout Namurian times
448 by unit thickness variations (e.g. Read, 1988; Chadwick *et al.*, 1995), perhaps suggesting pre-

449 Westphalian NE-SW dextral transpression (e.g. Underhill *et al.*, 2008). The preferential intrusion of
450 Early Permian igneous material along tensile and approximately ENE- and WNW-orientated faults
451 and pre-Permian normal activation of these faults perhaps suggests post-Westphalian and
452 Stephanian NE-SW dextral transtension (e.g. De Paola *et al.*, 2005).

453 *7.2 Strain localisation along obliquely orientated structures*

454 Given the important role that faulting, folding and positive inversion appears to have played
455 in determining the characteristics of late Carboniferous depocentres in the Canonbie Coalfield, we
456 consider the localisation of strain along depocentre defining structures. In northern Britain, the
457 localisation of strain along obliquely orientated structural trends with respect to the apparent,
458 approximately N-S compressional stress orientation requires fault damage zones significantly weaker
459 (>30 %) than intact bedrock (Copley and Woodcock, 2016). Having possibly undergone reverse
460 (dextral) reactivation during Namurian times and reverse reactivation during deposition of the
461 PMCM, albeit only partial reactivation along fault length (Fig. 6), NE-SW trending faults such as the
462 Gilnockie Fault are likely to have remained susceptible to further reverse reactivation, even in a
463 contrasting lateral sense, during deposition of the Warwickshire Group. There is limited evidence to
464 suggest that approximately E-W trending structures that were roughly perpendicular to the
465 orientation of maximum compressional stress, at Canonbie or in the immediately surrounding
466 region, accommodated significant basin shortening during this period (Fig. 6) (De Paola *et al.*, 2005).
467 Three-dimensional sandbox models and modern day analogues for inverted basins suggest that
468 steep faults orientated perpendicular to the orientation of maximum compressive stress are unlikely
469 to accommodate significant shortening in low-strain settings (Keller and McClay, 1995; Di Domenica
470 *et al.*, 2014). With this in mind, E-W structures that were perpendicular with respect to
471 compressional stress, may have remained 'frozen' during this period, leaving more oblique, recently
472 active and, therefore, mechanically weaker structures to accommodate preferential shortening.

473 *7.3 Strain location within rheologically weaker crustal rock*

474 Line-length restoration suggests that at least 10 % cumulative shortening occurred along a
475 NW-SE axis throughout the prolonged late Carboniferous inversion phase (Fig. 9). In reality, basin
476 shortening is likely to have been larger due to both sub-seismic scale shortening and out-of-plane
477 deformation. This shortening occurred in a region widely regarded as having occupied a low-strain
478 setting within the Carboniferous foreland (Corfield *et al.*, 1996; De Paola *et al.*, 2005). In the Midland
479 Valley of Scotland, steeply dipping faults such as the Highland Boundary and Southern Upland fault
480 systems are believed to have exerted a strong control on the magnitude of shortening (Ritchie *et al.*,
481 2003; Underhill *et al.*, 2008). A dissipating stress field derived from these faults may have
482 contributed towards the localised stress field at Canonbie. However, despite their shared proximities
483 to these fault systems, as well their similarly orientated structural fabrics, based on regional studies
484 subsurface studies and accounts of outcropping geology (*cf.* Chadwick *et al.*, 1995; Lumsden *et al.*,
485 1967), there is a large disparity between the high magnitude of basin shortening observed at
486 Canonbie compared with the Scottish Southern Uplands or the Lake District (Fig. 1). The Solway
487 Basin and the Canonbie Coalfield is underpinned by relatively weak upper crustal rock, composed
488 predominantly of thick Carboniferous sediment and weakly metamorphosed Ordovician-Silurian
489 slate and phyllite (Rickards and Woodcock, 2005; Stone *et al.*, 2012). This contrasts with the thinner
490 Carboniferous successions preserved immediately to the south and north of the coalfield that are
491 underpinned by mechanically strong granitoid basement rock in the Lake District and partially
492 granitic, greywacke dominant basement rock in the Southern Uplands of Scotland (Bott *et al.*, 1967;
493 Allsop *et al.*, 1987; Howell *et al.*, 2019, 2020). As a result, the Solway Basin may have therefore also
494 accommodated shortening for a wider region, including those mechanically stronger regions that
495 were less able to accommodate basin shortening, just as the Solway Basin likely accommodated
496 early Carboniferous extension for a wider region.

497 High magnitude seismic-scale folding and thrusting is often accommodated by a shallow to
498 mid-level crustal detachment (Coward *et al.*, 1999). The northwards dipping Iapetus suture zone
499 that, prior to Caledonian collision of Avalonia and Laurentia, separated present day Scotland from

500 northern England (*cf.* Freeman *et al.*, 1988; Soper *et al.*, 1992) constitutes such a detachment. This
501 detachment is undoubtedly at a relatively shallow depth beneath the Canonbie Coalfield and Solway
502 Basin, regardless of the contrasting interpolations of the onshore Iapetus suture zone (Fig. 1)
503 (Chadwick *et al.*, 1995; De Paola *et al.*, 2005). Furthermore, our cross-section restorations of the
504 Solway Syncline through the Canonbie Coalfield suggest a detachment at 6 to 7 km depth below
505 surface (Fig. 9) that may reflect this suture. Along with the locally mechanically weak crustal rock
506 underpinning the region, the favourable (slightly oblique) structural fabric orientation and the weak
507 (following dextral reactivation) accommodating NE-trending faults, this detachment may therefore
508 have also been able to aid the accommodation of greater localised basin shortening with respect to
509 adjacent areas.

510 *7.4 Implications for decarbonisation and low carbon subsurface energy resources in northern England* 511 *and southern Scotland*

512 Over the past century, coal including that sourced from the Canonbie Coalfield fuelled the
513 bulk of the UK's electricity and heating. Due to both the increased availability of domestic natural
514 gas and the UK's recent effort to decarbonise its energy supply, this is no longer the case. On the
515 contrary, the use of coal is widely condemned by western media as coal is now regarded as the
516 'dirtiest' fossil fuel because of the associated CO₂ and other pollutant emissions. However, UK coal
517 mining has left a legacy of abandoned infrastructure that has the potential to be repurposed as the
518 UK seeks to further decarbonise its energy supply (Andrews *et al.*, 2020). At the time of writing, the
519 British Geological Survey are constructing and operating a research site in Glasgow to further
520 understand the potential of water from abandoned coalmines for geothermal energy (Watson *et al.*,
521 2019). Coupled CO₂ sequestration and enhanced coal bed methane recovery offers a further, if
522 riskier, low carbon subsurface energy prospect for northern England and southern Scotland (Jones *et*
523 *al.*, 2004). This technology remains in its infancy although the Canonbie Coalfield itself was
524 investigated as recently as 2015 for coal bed methane purposes. Development plans were
525 abandoned due to, amongst other factors, the 'structural complexity' of the coalfield. To date, three

526 deliberate deep geothermal wells have been drilled in neighbouring northern England, penetrating
527 Carboniferous strata (Gluyas *et al.*, 2018). Thus far, the most encouraging of these wells was the
528 Eastgate borehole which intersected high permeability basement faults and fractures (Manning *et*
529 *al.*, 2007). Carboniferous tectonism is widely believed to have been underpinned by steeply dipping
530 thick-skinned, basement involved faults such as those intersected by the Eastgate borehole (Corfield
531 *et al.*, 1996). Our cross-section restorations for the Canonbie Coalfield, however, suggest that
532 deformation in this area was instead accommodated by more shallowly dipping structures that are
533 sub-horizontal at *c.* 6-7 km depth. Given that this study has revealed inconsistencies between past
534 assumptions made regarding the bedrock that hosts these potential resources and reality, and that
535 investments such as those highlighted are already being made, would it therefore not be worth
536 investing time exploring pre-existing and publicly available datasets in order to reduce uncertainties
537 surrounding the UK subsurface?

538 **8. Conclusions**

- 539 • Local seismic and borehole-based mapping of the late Carboniferous succession in the
540 Canonbie Coalfield (SW Scotland) provides evidence of repeated episodes of positive
541 inversion, syn-depositional folding and unconformities within the Westphalian (Bashkirian-
542 Moscovian) to Stephanian (Kasimovian) Pennine Coal Measures and Warwickshire Group
543 successions.
- 544 • Positive inversion and syn-depositional folding dictated Westphalian-Stephanian
545 depocentres at Canonbie. The basin history thus revealed is at variance with generally
546 accepted models in neighbouring northern England that state these basins subsided due to
547 post-rift thermal subsidence during the late Carboniferous.
- 548 • A Stephanian (?) unconformity within the Warwickshire Group succession at Canonbie,
549 which approximately correlates with ~10 % local basin shortening, documented further
550 major basin shortening throughout the late Carboniferous Variscan foreland and the

551 formation of the Cantabrian and Iberian oroclinal in southern Europe, also contradicts
552 observations that maximum Variscan shortening at this time had minimal impact on late
553 Carboniferous basins in northern England.

554 • Our mapping of the Westphalian-Stephanian succession at Canonbie evokes similarities
555 between the local Variscan foreland basin system and 'broken' foreland systems, where
556 sedimentation is controlled by local tectonism, such as the North Patagonian broken
557 foreland in South America.

558 • Local variations in crustal rheology, inherited fault strengths and their variation over time,
559 fault orientation with respect to the evolving dominant stress field and mid-crustal
560 detachments are suggested to play important roles in strain localisation and ultimately the
561 nature of Westphalian-Stephanian depocentres at the Canonbie Coalfield.

562

563 **Acknowledgments**

564 We acknowledge with thanks the help and co-operation in Dr. Tim Pharoah (BGS) and the staff of
565 the National Geoscience Data Centre in locating the borehole velocity data for the British Coal
566 boreholes. Dr. Malcolm Butler (UKOGL) is thanked for facilitating access to the seismic data; Keith
567 Whitworth (formerly of British Coal) is thanked by providing a digital copy of the logs of Becklees
568 Borehole. We would like to also acknowledge constructive reviews on an earlier version of this
569 manuscript by Dr. David Millward and by Dr. Steven Corfield.

570

571 **Funding**

572 This manuscript contains work conducted during a PhD study undertaken as part of the Natural
573 Environment Research Council (NERC) Centre for Doctoral Training (CDT) in Oil & Gas [grant number:
574 NEM00578X/1]. It is sponsored by Natural Environment Research Council, the Keele University Acorn
575 Fund and the National Productivity Investment Fund (NPIF) whose support is gratefully
576 acknowledged.

577

578 **References**

- 579 Allsop, J.M., 1987. Patterns of late Caledonian intrusive activity in eastern and northern England from
580 geophysics, radiometric dating and basement geology. *Proceedings of the Yorkshire Geological*
581 *Society*, 46(4), pp.335-353. <https://doi.org/10.1144/pygs.46.4.335>
- 582 Andrews, B.J., Cumberpatch, Z.A., Shipton, Z.K. and Lord, R., 2020. Collapse processes in
583 abandoned pillar and stall coal mines: implications for shallow mine geothermal
584 energy. *Geothermics*, 88, p.101904. <https://doi.org/10.1016/j.geothermics.2020.101904>
- 585 Assumpcao, M., 1992. The regional intraplate stress field in South America. *Journal of Geophysical*
586 *Research: Solid Earth*, 97(B8), pp.11889-11903. <https://doi.org/10.1029/91JB01590>
- 587 Bea, F., Fershtater, G.B. and Montero, P., 2002. Granitoids of the Uralides: Implications for the
588 evolution of the orogen. *Washington DC American Geophysical Union Geophysical Monograph*
589 *Series*, 132, pp.211-232. <https://doi.org/10.1029/132GM11>
- 590 Besly, B.M., 1988. Palaeogeographic implications of late Westphalian to early Permian red-beds,
591 Central England. In: Besly, B.M., and Kelling, G., (Eds.), *Sedimentation in a synorogenic basin*
592 *complex. The Upper Carboniferous of Northwest Europe*. Blackie and Son, Glasgow, pp. 200-221.
- 593 Besly, B.M., Burley, S.D. and Turner, P., 1993, January. The late Carboniferous 'Barren Red Bed' play
594 of the Silver Pit area, Southern North Sea. In: *Geological Society, London, Petroleum Geology*
595 *Conference series* (Vol. 4, No. 1, pp. 727-740). Geological Society of London.
596 <https://doi.org/10.1144/0040727>
- 597 Besly, B.M. and Cleal, C.J., 1997. Upper Carboniferous stratigraphy of the West Midlands (UK)
598 revised in the light of borehole geophysical logs and detrital compositional suites. *Geological*
599 *Journal*, 32(2), pp.85-118. [https://doi.org/10.1002/\(SICI\)1099-1034\(199706\)32:2<85::AID-
600 \[GJ732>3.0.CO;2-O\]\(https://doi.org/10.1002/\(SICI\)1099-1034\(199706\)32:2<85::AID-GJ732>3.0.CO;2-O\)](https://doi.org/10.1002/(SICI)1099-1034(199706)32:2<85::AID-GJ732>3.0.CO;2-O)
- 601 Besly, B., 2019. Exploration and development in the Carboniferous of the Southern North Sea: a 30-
602 year retrospective. *Geological Society, London, Special Publications*, 471(1), pp.17-64.
603 <https://doi.org/10.1144/SP471.10>Besly, B. M. and Cleal, C. J., in press. Regional stratigraphic hiatus

604 in the late Carboniferous (Asturian-Stephanian) in the northern Variscan foreland: a review of the bio-
605 and lithostratigraphical evidence in central England.

606 Bilmes, A., D'Elia, L., Franzese, J.R., Veiga, G.D. and Hernández, M., 2013. Miocene block uplift and
607 basin formation in the Patagonian foreland: the Gastre Basin, Argentina. *Tectonophysics*, 601, pp.98-
608 111. <https://doi.org/10.1016/j.tecto.2013.05.001>

609 Bott, M.H.P., 1967. Geophysical investigations of the northern Pennine basement rocks. *Proceedings*
610 *of the Yorkshire Geological Society*, 36(2), pp.139-168. <https://doi.org/10.1144/pygs.36.2.139>

611 Brown, D., Juhlin, C., Tryggvason, A., Friberg, M., Rybalka, A., Puchkov, V. and Petrov, G., 2006.
612 Structural architecture of the southern and middle Urals foreland from reflection seismic
613 profiles. *Tectonics*, 25(1). <https://doi.org/10.1029/2005TC001834>

614 Bucher, J., García, M., López, M., Milanese, F., Bilmes, A., D'Elia, L., Naipauer, M., Sato, A.M.,
615 Funes, D., Rapalini, A. and Franzese, J.R., 2019. Tectonostratigraphic evolution and timing
616 deformation in the Miocene Paso del Sapo Basin: Implications for the Patagonian broken
617 foreland. *Journal of South American Earth Sciences*, 94, p.102212.
618 <https://doi.org/10.1016/j.jsames.2019.102212>

619 Burgess, P.M. and Gayer, R.A., 2000. Late Carboniferous tectonic subsidence in South Wales:
620 implications for Variscan basin evolution and tectonic history in SW Britain. *Journal of the Geological*
621 *Society*, 157(1), pp.93-104. <https://doi.org/10.1144/jgs.157.1.93>

622 Butler, M., 1998. The geological history of the southern Wessex Basin—a review of new information
623 from oil exploration. *Geological Society, London, Special Publications*, 133(1), pp.67-86.
624 <https://doi.org/10.1144/GSL.SP.1998.133.01.04>

625 Butler, M., 2019. Seismostratigraphic analysis of Paleozoic sequences of the Midlands
626 Microcraton. *Geological Society, London, Special Publications*, 471(1), pp.317-332.
627 <https://doi.org/10.1144/SP471.6>

628 Caldwell, W.G.E. and Young, G.M., 2013. Structural controls in the
629 western offshore Midland Valley of Scotland: implications for Late Palaeozoic regional
630 tectonics. *Geological Magazine*, 150(4), pp.673-698. <https://doi.org/10.1017/S0016756812000878>

631 Cameron, I.B. and Stephenson, D., 1985. *British Regional Geology: The Midland Valley of*
Scotland (Fifth edition). London: HMSO.

632 Catuneanu, O., 2019. First-order foreland cycles: Interplay of flexural tectonics, dynamic loading, and
633 sedimentation. *Journal of Geodynamics*, 129, pp.290-298. <https://doi.org/10.1016/j.jog.2018.03.001>

634 Chadwick, B.A., Holliday, D.W., Holloway, S., Hulbert, A.G. and Lawrence, D.J.D., 1995. The
635 structure and evolution of the Northumberland-Solway Basin and adjacent areas. *Subsurface memoir*
636 *of the British Geological Survey*. London: HMSO.

637 Clarke, W.J., 1901. The Unconformity in the Coal-Measures of the Shropshire Coalfields. *Quarterly*
638 *Journal of the Geological Society*, 57(1-4), pp.86-95.

639 Corfield, S.M., Gawthorpe, R.L., Gage, M., Fraser, A.J. and Besly, B.M., 1996. Inversion tectonics of
640 the Variscan foreland of the British Isles. *Journal of the Geological Society*, 153(1), pp.17-32.
641 <https://doi.org/10.1144/gsjgs.153.1.0017>

642 Copley, A., Avouac, J.P. and Wernicke, B.P., 2011. Evidence for mechanical coupling and strong
643 Indian lower crust beneath southern Tibet. *Nature*, 472(7341), pp.79-81.
644 <https://doi.org/10.1038/nature09926>

645 Copley, A. and Woodcock, N., 2016. Estimates of fault strength from the Variscan foreland of the
646 northern UK. *Earth and Planetary Science Letters*, 451, pp.108-113.
647 <https://doi.org/10.1016/j.epsl.2016.07.024>

648 Coward, M.P., 1993. The effect of Late Caledonian and Variscan continental escape tectonics on
649 basement structure, Paleozoic basin kinematics and subsequent Mesozoic basin development in NW
650 Europe. In *Geological Society, London, Petroleum Geology Conference series* (Vol. 4, No. 1, pp.
651 1095-1108). Geological Society of London. <https://doi.org/10.1144/0041095>

652 Coward, M.P., De Donatis, M., Mazzoli, S., Paltrinieri, W. and Wezel, F.C., 1999. Frontal part of the
653 northern Apennines fold and thrust belt in the Romagna-Marche area (Italy): Shallow and deep
654 structural styles. *Tectonics*, 18(3), pp.559-574. <https://doi.org/10.1029/1999TC900003>

655 Crampton, S.L. and Allen, P.A., 1995. Recognition of forebulge unconformities associated with early
656 stage foreland basin development: example from the North Alpine Foreland Basin. *AAPG*
657 *bulletin*, 79(10), pp.1495-1514.

658 Creedy, D.P., 1991. An introduction to geological aspects of methane occurrence and control in
659 British deep coal mines. *Quarterly Journal of Engineering Geology and Hydrogeology*, 24(2), pp.209-
660 220. <https://doi.org/10.1144/GSL.QJEG.1991.024.02.04>

661 Davydov V., Wardlaw B.R., Gradstein F.M., 2004. *The Carboniferous Period*. In: Gradstein F.M., Ogg
662 J.G., Smith A.G., (Eds.). *A geologic time scale 2004*. Cambridge: Cambridge University Press. p.
663 222–248.

664 Dean, M.T., Browne, M.A.E., Waters, C.N., and Powell, J.H., 2011. *A lithostratigraphical framework*
665 *for the Carboniferous successions of northern Great Britain (Onshore)*. British Geological Survey
666 Research Report, RR/10/07. 174pp.

667 DeCelles, P.G. and Giles, K.A., 1996. Foreland basin systems. *Basin research*, 8(2), pp.105-123.
668 <https://doi.org/10.1046/j.1365-2117.1996.01491.x>

669 DeCelles, P.G., 2012. Foreland basin systems revisited: Variations in response to tectonic
670 settings. *Tectonics of sedimentary basins: Recent advances*, pp.405-426.
671 <https://doi.org/10.1002/9781444347166.ch20>

672 Dempsey, E. 2016. The North Pennines Orefield: a major regional phase of mantle sourced
673 mineralisation, magmatism and transtension during the earliest Permian. *Proceedings of the Open*
674 *University Geological Society*, 2, pp. 33-37.

675 De Paola, N., Holdsworth, R.E., McCaffrey, K.J. and Barchi, M.R., 2005. Partitioned transtension: an
676 alternative to basin inversion models. *Journal of Structural Geology*, 27(4), pp.607-625.
677 <https://doi.org/10.1016/j.jsg.2005.01.006>

678 Di Domenica, A., Bonini, L., Calamita, F., Toscani, G., Galuppo, C. and Seno, S., 2014. Analogue
679 modeling of positive inversion tectonics along differently oriented pre-thrusting normal faults: an
680 application to the Central-Northern Apennines of Italy. *Bulletin*, 126(7-8), pp.943-955.
681 <https://doi.org/10.1130/B31001.1>

682 Domeier, M. and Torsvik, T.H., 2014. Plate tectonics in the late Paleozoic. *Geoscience Frontiers*, 5(3),
683 pp.303-350. <https://doi.org/10.1016/j.gsf.2014.01.002>

684 Edel, J.B., Schulmann, K., Lexa, O. and Lardeaux, J.M., 2018. Late Palaeozoic palaeomagnetic and
685 tectonic constraints for amalgamation of Pangaea supercontinent in the European Variscan
686 belt. *Earth-science reviews*, 177, pp.589-612. <https://doi.org/10.1016/j.earscirev.2017.12.007>

687 Ellen, R., Browne, M.A.E., Mitten, A.J., Clarke, S.M., Leslie, A.G. and Callaghan, E., 2019.
688 Sedimentology, architecture and depositional setting of the fluvial Spireslack Sandstone of the
689 Midland Valley, Scotland: insights from the Spireslack surface coal mine. *Geological Society, London,*
690 *Special Publications*, 488, pp.SP488-2. <https://doi.org/10.1144/SP488.2>

691 Evans, D.J., Rowley, W.J., Chadwick, R.A., Kimbell, G.S. and Millward, D., 1994. Seismic reflection
692 data and the internal structure of the Lake District batholith, Cumbria, northern England. *Proceedings*
693 *of the Yorkshire Geological Society*, 50(1), pp.11-24. <https://doi.org/10.1144/pygs.50.1.11>

694 Fraser, A.J. and Gawthorpe, R.L., 1990. Tectono-stratigraphic development and hydrocarbon habitat
695 of the Carboniferous in northern England. *Geological Society, London, Special Publications*, 55(1),
696 pp.49-86. <https://doi.org/10.1144/GSL.SP.1990.055.01.03>

697 Freeman, B., Klemperer, S.L. and Hobbs, R.W., 1988. The deep structure of northern England and
698 the Iapetus Suture zone from BIRPS deep seismic reflection profiles. *Journal of the Geological*
699 *Society*, 145(5), pp.727-740. <https://doi.org/10.1144/gsjgs.145.5.0727>

700 Gianni, G., Navarrete, C., Orts, D., Tobal, J., Folguera, A. and Giménez, M., 2015. Patagonian broken
701 foreland and related synorogenic rifting: the origin of the Chubut Group Basin. *Tectonophysics*, 649,
702 pp.81-99. <https://doi.org/10.1016/j.tecto.2015.03.006>

703 Hirst, C., Manning, D.A.C., McCay, A., Narayan, N.S., Robinson, H.L., Watson, S.M. and Westaway,
704 R., 2018. Keeping warm: a review of deep geothermal potential of the UK. *Proceedings of the*
705 *Institution of Mechanical Engineers, Part A: Journal of Power and Energy*, 232(1), pp.115-126.
706 <https://doi.org/10.1177/0957650917749693>

707 Gochioco, L.M., 1990. Seismic surveys for coal exploration and mine planning. *The Leading*
708 *Edge*, 9(4), pp.25-28. <https://doi.org/10.1190/1.1439738>

709 Green, P.F., 1986. On the thermo-tectonic evolution of Northern England: evidence from fission track
710 analysis. *Geological Magazine*, 123(5), pp.493-506. <https://doi.org/10.1017/S0016756800035081>

711 Hayward, A.B. and Graham, R.H., 1989. Some geometrical characteristics of inversion. *Geological*
712 *Society, London, Special Publications*, 44(1), pp.17-39.
713 <https://doi.org/10.1144/GSL.SP.1989.044.01.03>

714 Howell, L., Egan, S., Leslie, G. and Clarke, S., 2019. Structural and geodynamic modelling of the
715 influence of granite bodies during lithospheric extension: application to the Carboniferous basins of
716 northern England. *Tectonophysics*, 755, pp.47-63. <https://doi.org/10.1016/j.tecto.2019.02.008>

717 Howell, L., Egan, S., Leslie, G., Clarke, S., Mitten, A. and Pringle, J., 2020. The influence of low-
718 density granite bodies on extensional basins. *Geology Today*, 36(1), pp. 22-26.
719 <https://doi.org/10.1111/gto.12297>

720 Jackson, C.L., Chua, S.T., Bell, R.E. and Magee, C., 2013. Structural style and early stage growth of
721 inversion structures: 3D seismic insights from the Egersund Basin, offshore Norway. *Journal of*
722 *Structural Geology*, 46, pp.167-185. <https://doi.org/10.1016/j.jsg.2012.09.005>

723 Jones N.S., Holloway S., Creedy D.P., Garner K., Smith N.J.P., Browne, M.A.E. and Durucan S.
724 2004. UK Coal Resource for New Exploitation Technologies. Final Report. British Geological Survey
725 Commissioned Report CR/04/015N.

726 Jones, N.S. and Holliday, D.W., 2016. Intra-Carboniferous deformation and unconformity at Gilnockie
727 Bridge, SW Scotland, reinterpreted as the result of multiple channel-bank collapse. *Scottish Journal of*
728 *Geology*, 52(1), pp.43-54. <https://doi.org/10.1144/sjg2015-009>

729 Jones, N. S. and Holliday, D. W., 2006. The stratigraphy and sedimentology of Upper Carboniferous
730 Warwickshire Group red-bed facies in the Canonbie area of S.W. Scotland. British Geological Survey
731 Internal Report, IR/06/043. 75pp.

732 Jones, N.S., Holliday, D.W. and McKervey, J.A., 2011. Warwickshire Group (Pennsylvanian) red-beds
733 of the Canonbie Coalfield, England–Scotland border, and their regional palaeogeographical
734 implications. *Geological Magazine*, 148(1), pp.50-77. <https://doi.org/10.1017/S001675681000035X>

735 Karner, G.D. and Watts, A.B., 1983. Gravity anomalies and flexure of the lithosphere at mountain
736 ranges. *Journal of Geophysical Research: Solid Earth*, 88(B12), pp.10449-10477.
737 <https://doi.org/10.1029/JB088iB12p10449>

738 Keller, J.V.A. and McClay, K.R., 1995. 3D sandbox models of positive inversion. *Geological Society,*
739 *London, Special Publications*, 88(1), pp.137-146. <https://doi.org/10.1144/GSL.SP.1995.088.01.09>

740 Kimbell, G.S., Chadwick, R.A., Holliday, D.W. and Werngren, O.C., 1989. The structure and evolution
741 of the Northumberland Trough from new seismic reflection data and its bearing on modes of
742 continental extension. *Journal of the Geological Society*, 146(5), pp.775-787.
743 <https://doi.org/10.1144/gsjgs.146.5.0775>

744 Leeder, M.R., 1982. Upper Palaeozoic basins of the British Isles—Caledonide inheritance versus
745 Hercynian plate margin processes. *Journal of the Geological Society*, 139(4), pp.479-491.
746 <https://doi.org/10.1144/gsjgs.139.4.0479>

747 Leslie, A.G., Millward, D., Pharaoh, T., Monaghan, A.A., Arsenikos, S. and Quinn, M., 2015. Tectonic
748 synthesis and contextual setting for the Central North Sea and adjacent onshore areas, 21CXR
749 Palaeozoic Project.

750 Liu, S., Nummedal, D. and Liu, L., 2011. Migration of dynamic subsidence across the Late
751 Cretaceous United States Western Interior Basin in response to Farallon plate
752 subduction. *Geology*, 39(6), pp.555-558. <https://doi.org/10.1130/G31692.1>

753 López, M., García, M., Bucher, J., Funes, D.S., D'Elia, L., Bilmes, A., Naipauer, M., Sato, A.M.,
754 Valencia, V.A. and Franzese, J.R., 2019. Structural evolution of The Collón Cura basin: Tectonic
755 implications for the north Patagonian Broken Foreland. *Journal of South American Earth*
756 *Sciences*, 93, pp.424-438. <https://doi.org/10.1016/j.jsames.2019.04.021>

757 Lumsden, G.I., Tulloch, W., Howells, M.F., Davies, A., Wilson, R.B., Calver, M.A., Smith, J.D.D. and
758 Elliot, R.W., 1967. The geology of the neighbourhood of Langholm: Explanation of one-inch geological
759 sheet (Vol. 11). *Memoirs of the Geological Survey of Great Britain (Scotland)*. HMSO, Edinburgh.
760 <http://pubs.bgs.ac.uk/publications.html?pubID=B01863>

761 Manning, D.A.C., Younger, P.L., Smith, F.W., Jones, J.M., Dufton, D.J. and Diskin, S., 2007. A deep
762 geothermal exploration well at Eastgate, Weardale, UK: a novel exploration concept for low-enthalpy
763 resources. *Journal of the Geological Society*, 164(2), pp.371-382. [https://doi.org/10.1144/0016-](https://doi.org/10.1144/0016-76492006-015)
764 [76492006-015](https://doi.org/10.1144/0016-76492006-015)

765 McKenzie, D., 1978. Some remarks on the development of sedimentary basins. *Earth and Planetary*
766 *science letters*, 40(1), pp.25-32. [https://doi.org/10.1016/0012-821X\(78\)90071-7](https://doi.org/10.1016/0012-821X(78)90071-7)

767 Monaghan, A.A. and Pringle, M.S., 2004. 40Ar/39Ar geochronology of Carboniferous-Permian
768 volcanism in the Midland Valley, Scotland. *Geological Society, London, Special Publications*, 223(1),
769 pp.219-241. <https://doi.org/10.1144/GSL.SP.2004.223.01.10>

770 Murphy, J.B., Quesada, C., Gutiérrez-Alonso, G., Johnston, S.T. and Weil, A., 2016. Reconciling
771 competing models for the tectono-stratigraphic zonation of the Variscan orogen in Western
772 Europe. *Tectonophysics*, 681, pp.209-219. <https://doi.org/10.1016/j.tecto.2016.01.006>

773 Mykura, W., Calver, M.A. and Wilson, R.B., 1967. The Upper Carboniferous rocks of south-west
774 Ayrshire. *Bulletin of the Geological Survey of Great Britain*, 26, pp.23-98. Nance, R.D., Gutiérrez-
775 Alonso, G., Keppie, J.D., Linnemann, U., Murphy, J.B., Quesada, C., Strachan, R.A. and Woodcock,
776 N.H., 2012. A brief history of the Rheic Ocean. *Geoscience Frontiers*, 3(2), pp.125-135.

777 Peace, G.R. and Besly, B.M., 1997. End-Carboniferous fold-thrust structures, Oxfordshire, UK:
778 implications for the structural evolution of the late Variscan foreland of south-central England. *Journal*
779 *of the Geological Society*, 154(2), pp.225-237. <https://doi.org/10.1144/gsjgs.154.2.0225>

780 Pharaoh, T., Haslam, R., Hough, E., Kirk, K., Leslie, G., Schofield, D. and Heafford, A., 2019. The
781 Môn-Deemster-Ribblesdale Fold-Thrust Belt, Central UK: a concealed variscan inversion belt located
782 on weak caledonian crust. *Geological Society, London, Special Publications*, 490, pp.SP490-2018.
783 <https://doi.org/10.1144/SP490-2018-109>

784 Picken, G.S., 1988. The concealed coalfield at Canonbie: an interpretation based on boreholes and
785 seismic surveys. *Scottish Journal of Geology*, 24(1), pp.61-71. <https://doi.org/10.1144/sjg24010061>

786 Poole, E.G., 1988. The concealed coalfield of Canonbie: Comment. *Scottish Journal of*
787 *Geology*, 24(3), pp.305-306. <https://sjg.lyellcollection.org/content/sjg/24/3/305.full.pdf>

788 Powell, J.H., Chisholm, J.I., Bridge, D.M., Rees, J.G., Glover, B.W. and Besly, B.M., 2000.
789 Stratigraphical framework for Westphalian to Early Permian red-bed successions of the Pennine
790 Basin. *British Geological Survey Research Report*, RR/00/01.

791 Powers, P.M., Lillie, R.J. and Yeats, R.S., 1998. Structure and shortening of the Kangra and Dehra
792 Dun reentrants, sub-Himalaya, India. *Geological Society of America Bulletin*, 110(8), pp.1010-1027.
793 [https://doi.org/10.1130/0016-7606\(1998\)110<1010:SASOTK>2.3.CO;2](https://doi.org/10.1130/0016-7606(1998)110<1010:SASOTK>2.3.CO;2)

794 Ramos, E., Busquets, P. and Vergés, J., 2002. Interplay between longitudinal fluvial and transverse
795 alluvial fan systems and growing thrusts in a piggyback basin (SE Pyrenees). *Sedimentary*
796 *Geology*, 146(1-2), pp.105-131. [https://doi.org/10.1016/S0037-0738\(01\)00169-5](https://doi.org/10.1016/S0037-0738(01)00169-5)

797 Read, W.A., 1988. Controls on Silesian sedimentation in the Midland Valley of Scotland. In: Besly,
798 B.M., Kelling, G. (Eds.), *Sedimentation in a Synorogenic Basin Complex: the Upper Carboniferous of*
799 *Northwest Europe*. Blackie and Son, Glasgow, pp. 222–241.

800 Rickards, R.B. and Woodcock, N.H., 2005. Stratigraphical revision of the Windermere Supergroup
801 (Late Ordovician–Silurian in the southern Howgill Fells, NW England. *Proceedings of the Yorkshire*
802 *Geological Society*, 55(4), pp.263-285. <https://doi.org/10.1144/pygs.55.4.263>

803 Ritchie, J.D., Johnson, H., Browne, M.A.E. and Monaghan, A.A., 2003. Late Devonian–Carboniferous
804 tectonic evolution within the Firth of Forth, Midland Valley; as revealed from 2D seismic reflection
805 data. *Scottish Journal of Geology*, 39(2), pp.121-134. <https://doi.org/10.1144/sjg39020121>

806 Shaw, J. and Johnston, S.T., 2016. Oroclinal buckling of the Armorican ribbon continent: An
807 alternative tectonic model for Pangaeon amalgamation and Variscan orogenesis. *Lithosphere*, 8(6),
808 pp.769-777. <https://doi.org/10.1130/L559.1>

809 Song, T., 1997. Inversion styles in the Songliao basin (northeast China) and estimation of the degree
810 of inversion. *Tectonophysics*, 283(1-4), pp.173-188. [https://doi.org/10.1016/S0040-1951\(97\)00147-9](https://doi.org/10.1016/S0040-1951(97)00147-9)

811 Soper, N.J., England, R.W., Snyder, D.B. and Ryan, P.D., 1992. The Iapetus suture zone in England,
812 Scotland and eastern Ireland: a reconciliation of geological and deep seismic data. *Journal of the*
813 *Geological Society*, 149(5), pp.697-700. <https://doi.org/10.1144/gsjgs.149.5.0697>

814 Stone, P., McMillan, A.A., Floyd, J.D., Barnes, R.P. and Phillips, E.R., 2012. *British Regional*
815 *Geology: South of Scotland* (Fourth edition). Keyworth, Nottingham: British Geological Survey.

816 Strecker, M.R., Hilley, G.E., Bookhagen, B. and Sobel, E.R., 2011. Structural, geomorphic, and
817 depositional characteristics of contiguous and broken foreland basins: examples from the eastern

818 flanks of the central Andes in Bolivia and NW Argentina. *Tectonics of sedimentary basins: Recent*
819 *advances*, pp.508-521. <https://doi.org/10.1002/9781444347166.ch25>

820 Suriano, J., Limarino, C.O., Tedesco, A.M. and Alonso, M.S., 2015. Sedimentation model of
821 piggyback basins: Cenozoic examples of San Juan Precordillera, Argentina. *Geological Society,*
822 *London, Special Publications*, 399(1), pp.221-244. <https://doi.org/10.1144/SP399.17>

823 Underhill, J.R. and Brodie, J.A., 1993. Structural geology of Easter Ross, Scotland: implications for
824 movement on the Great Glen fault zone. *Journal of the Geological Society*, 150(3), pp.515-527.
825 <https://doi.org/10.1144/gsjgs.150.3.0515>

826 Underhill, J.R., Monaghan, A.A. and Browne, M.A., 2008. Controls on structural styles, basin
827 development and petroleum prospectivity in the Midland Valley of Scotland. *Marine and Petroleum*
828 *Geology*, 25(10), pp.1000-1022. <https://doi.org/10.1016/j.marpetgeo.2007.12.002>

829 Warr, L.N., 2012. The Variscan Orogeny: the welding of Pangaea. In: Woodcock, N. and Strachan R.
830 (Eds.) *Geological history of Britain and Ireland*. Wiley-Blackwell.

831 Waters, C.N, Browne, M.A.E, Dean, M.T, and Powell, J.H, 2007. *Lithostratigraphical framework for*
832 *Carboniferous successions of Great Britain (Onshore)*. British Geological Survey Research Report,
833 RR/07/01. 60pp.

834 Waters, C.N., Somerville, I.D., Stephenson, M.H., Cleal, C.J., Long, S. L. 2011. Biostratigraphy. In: *A*
835 *Revised Correlation of Carboniferous Rocks in the British Isles*, C. N. Waters; I. D. Somerville; N. S.
836 Jones; C. J. Cleal; J. D. Collinson; R. A. Waters; B. M. Besly; M. T. Dean; M. H. Stephenson; J. R.
837 Davies; E. C. Freshney; D. I. Jackson; W. I. Mitchell; J. H. Powell; W. J. Barclay; M. A. E. Browne; B.
838 E. Leveridge; S. L. Long; D. McLean (Eds.), Special Report 26. The Geological Society: London; 11–
839 22. <https://doi.org/10.1144/SR26>

840 Watson, S.M., Westaway, R. and Burnside, N.M., 2019. Digging deeper: The influence of historical
841 mining on Glasgow's subsurface thermal state to inform geothermal research.
842 <https://doi.org/10.1144/sjq2019-012>

843 Williams, G.D., Powell, C.M. and Cooper, M.A., 1989. Geometry and kinematics of inversion
844 tectonics. *Geological Society, London, Special Publications*, 44(1), pp.3-15.
845 <https://doi.org/10.1144/GSL.SP.1989.044.01.02>

846 Woodcock, N.H. and Rickards, B., 2003. Transpressive duplex and flower structure: Dent fault
847 system, NW England. *Journal of Structural Geology*, 25(12), pp.1981-1992.
848 [https://doi.org/10.1016/S0191-8141\(03\)00057-9](https://doi.org/10.1016/S0191-8141(03)00057-9)

849 Ziegler, P.A., 1993. Late Palaeozoic—Early Mesozoic plate reorganization: Evolution and demise of
850 the Variscan Fold Belt. In *Pre-Mesozoic geology in the Alps* (pp. 203-216). Springer, Berlin,
851 Heidelberg.

852

853 **Figure 1**

854 Fig. 1: (top) A simplified onshore geological map of northern Britain depicting the outcropping
855 Carboniferous succession. Major compressional structures are annotated in bold, many of which in
856 northern England and southern Scotland are oblique with respect to roughly north-south orientated
857 Variscan compressional stress (Corfield *et al.*, 1996). Numbered annotations indicate areas of
858 northern Britain where Warwickshire Group (or age equivalent stratigraphy) has been observed
859 cropping out (Powell *et al.*, 2000; Waters *et al.*, 2007; Jones *et al.*, 2011) (also see Fig. 3). MVS =
860 Midland Valley of Scotland; M-LS = Midlothian-Leven Syncline; BA = Bewcastle Anticline; SS = Solway
861 Syncline; DF = Dent Fault; MD FTB = Mòn-Deemster Fold and Thrust Belt. Mapping data courtesy of
862 the British Geological Survey. (bottom) A schematic NE-SW cross-section from the Southern Uplands,
863 through the Solway Basin and to the Lake District.

864

865 **Figure 2**

866 Fig. 2: A summary of the seismic and borehole data from the Canonbie Coalfield used in this study.

867 All seismic data was accessed through UKOGL (UK Onshore Geophysical Library). Borehole data was

868 accessed through the UK OGA (Oil and Gas Authority), IHS Markit and the BGS's (British Geological

869 Survey) archives at Keyworth.

870

871 **Figure 3**

872 Fig. 3a: (left) Stratigraphic columns showing international and regional Stage units of the late
873 Carboniferous. (right) Chronostratigraphic correlation of the Pennine and Scottish Coal Measures,
874 and Warwickshire Group from the Canonbie coalfield to southern Scotland, north-west England and
875 the English Midlands. Based primarily on petrographical work conducted by Jones *et al.* (2006;
876 2011), augmented by the seismic and regional interpretations of this study and data presented in
877 Picken (1988), Powell *et al.* (2000) and Waters *et al.* (2007). The correlation of regional
878 Carboniferous stages of Davydov (2004) is adopted, along with the palynozone subdivisions of
879 Waters *et al.* (2011). SLCM = Scottish Lower Coal Measures (Fm.); SMCM = Scottish Middle Coal
880 Measures; SUCM = Scottish Upper Coal Measures; PLCM = Pennine Lower Coal Measures; PUCM =
881 Pennine Upper Coal Measures; Esk. = Eskbank Wood; Can. = Canonbie Bridge Sandstone; Beck. =
882 Becklees Sandstone; WSF = Whitehaven Sandstone Formation; WSM = Whitehaven Sandstone
883 Member; MBM = Millyeat Beds Member. 3b: Locations of chronostratigraphically correlated Scottish
884 Coal Measures, and Warwickshire Group successions in the British Isles and relative to the late
885 Carboniferous Variscan thrust front (location of thrust front taken from Corfield *et al.*, 1996). 3c:
886 Depth correlations for the Pennine and Scottish Coal Measures, and Warwickshire Group from the
887 Canonbie coalfield to southern Scotland, north-west England and the English Midlands. Unit
888 thicknesses are taken from Waters *et al.* (2011). The Clent Formation and Kennilworth Sandstone
889 Formation (in green) are those interpreted by Peace and Besly (1997) to have been deposited after
890 an alleged final phase of Variscan inversion tectonics in the English Midlands.

891

892 **Figure 4**

893 Fig. 4: (left) Stratigraphic columns showing international and regional Stage units. (right) A seismic
894 well tie for the Becklees borehole. Gamma ray, density, sonic and lithological logs (based on Jones
895 and Holliday, 2006; Jones *et al.*, 2011) are shown along with synthetic and observed seismic traces. A
896 = Langsettian; B = Duckmantian; C = Bolsovian; D = Asturian; Gr. = Group; Fm. = Formation; TVD =
897 True Vertical Depth.

898

899 **Figure 5**

900 Fig. 5: Depth map to base Pennine Coal Measures Formation in metres in the Canonbie coalfield. The
901 dominant structural trends interpreted in the Canonbie Coalfield can be accounted for by dextral
902 wrenching along NE-SW orientated faults (inset top-left; 2D strain ellipse illustrating predicted
903 discontinuity trends after dextral wrench on NE-SW orientated faults). 5b, c and d: Isochore
904 thickness maps for the Pennine Lower, Middle and Upper Coal Measures Formations respectively,
905 based on the seismic interpretations of this study. Thickening during deposition of the Pennine
906 Middle and Upper Measures Formations is controlled dominantly by growth within the Solway
907 Syncline structure.

908

909 **Figure 6**

910 Fig. 6: An interpreted SW-NE orientated seismic profile from the Canonbie Coalfield (Seismic line
911 ED86-04), depicting normal faulting and strike-parallel plunge of the Solway Syncline. For section
912 location, see Figure 2. Uninterpreted profiles for all the seismic sections included in this study can be
913 previewed at ukogl.org.uk.

914

915 **Figure 7**

916 Fig. 7: A wireline (gamma ray) correlation panel for the late Carboniferous successions of the
917 Becklees, Glenzierfoot and Broadmeadows boreholes in the Canonbie Coalfield. Gamma ray curves
918 for the Glenzierfoot and Broadmeadows boreholes are derived from Jones *et al.* (2011). Gr. = Group;
919 Fm. = Formation; TVD = total vertical depth.

920 **Figure 8**

921 Fig. 8: An interpreted NW-SE seismic profile (Seismic line ED86-02) depicting folding of the Solway
922 Syncline, mild inversion along antithetic and synthetic normal faults of the Gilnockie Fault, onlapping
923 Pennine Middle Coal Measures (PMCM) against mild inversion folds and normal offset along the
924 Gilnockie Fault. For section location, see Fig. 2. Uninterpreted profiles for all the seismic sections
925 included in this study can be previewed at ukogl.org.uk.

926

927 **Figure 9**

928 Fig. 9a: An interpreted NW-SE orientated seismic profile depicting folding of the Solway Syncline
929 (Seismic line 80-CAN-54). 9b: A closer look at the reflector geometries belonging to the Becklees
930 Sandstone Formation (Warwickshire Group) within the axis of the Solway Syncline. A series of
931 reflectors are shown onlapping against the western limb of the Solway Syncline. Erosional truncation
932 of reflectors occurs within the axis of the Solway Syncline and is interpreted as representing down
933 cutting, fluvial strata. For section location, see Fig. 2. Uninterpreted profiles for all the seismic
934 sections included in this study can be previewed at ukogl.org.uk.

935

936 **Figure 10**

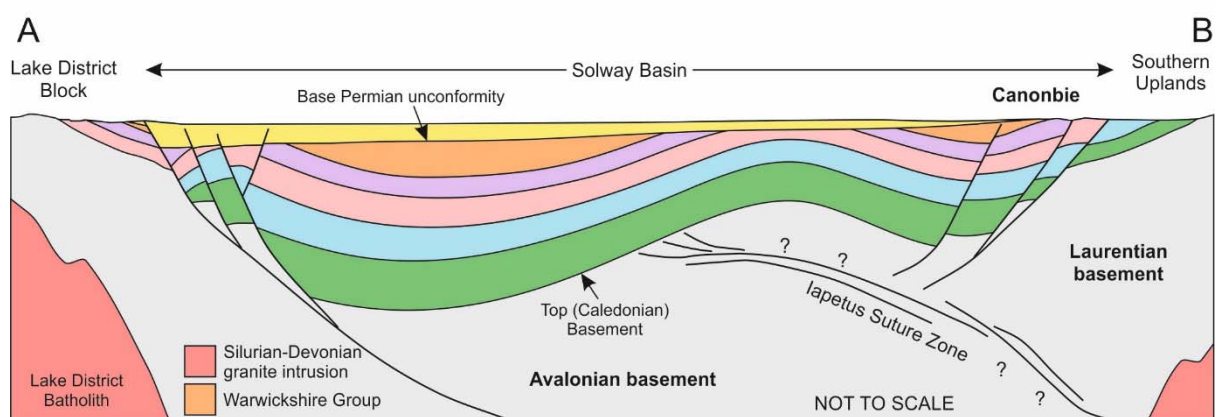
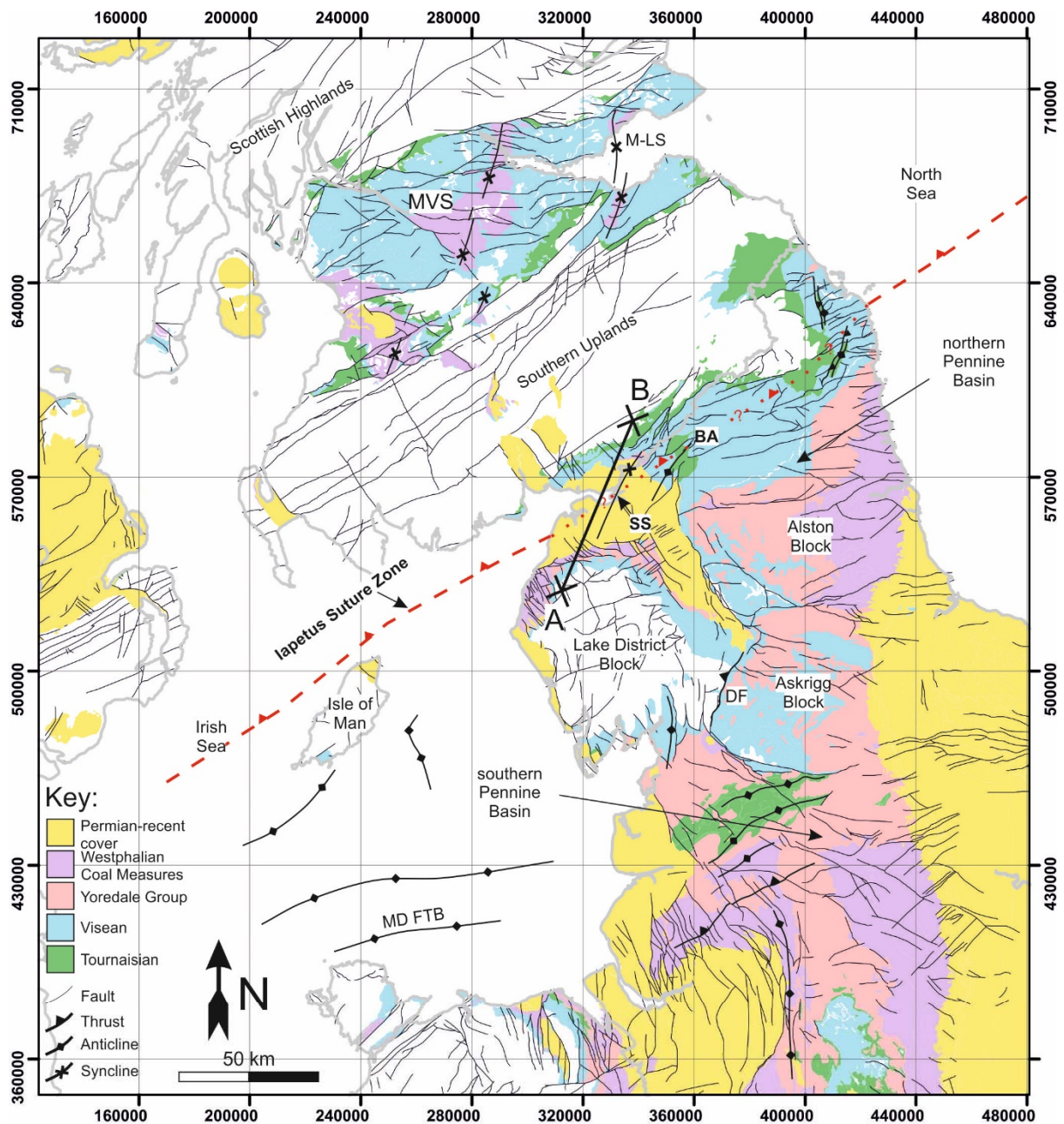
937 Fig. 10: Two-dimensional palinspastic cross-section restorations for the NW-SE orientated section
938 presented in Figure 9. Timings of deformation events are constrained by onlapping reflector
939 geometries. The cross-section can be restored by incorporating a sub-horizontal detachment at
940 around 6-7 km depth. Restorations are performed using the unfolding, move-on-fault and
941 decompaction modules in MOVE (Petroleum Experts) structural model building software.

942

943 **Figure 11**

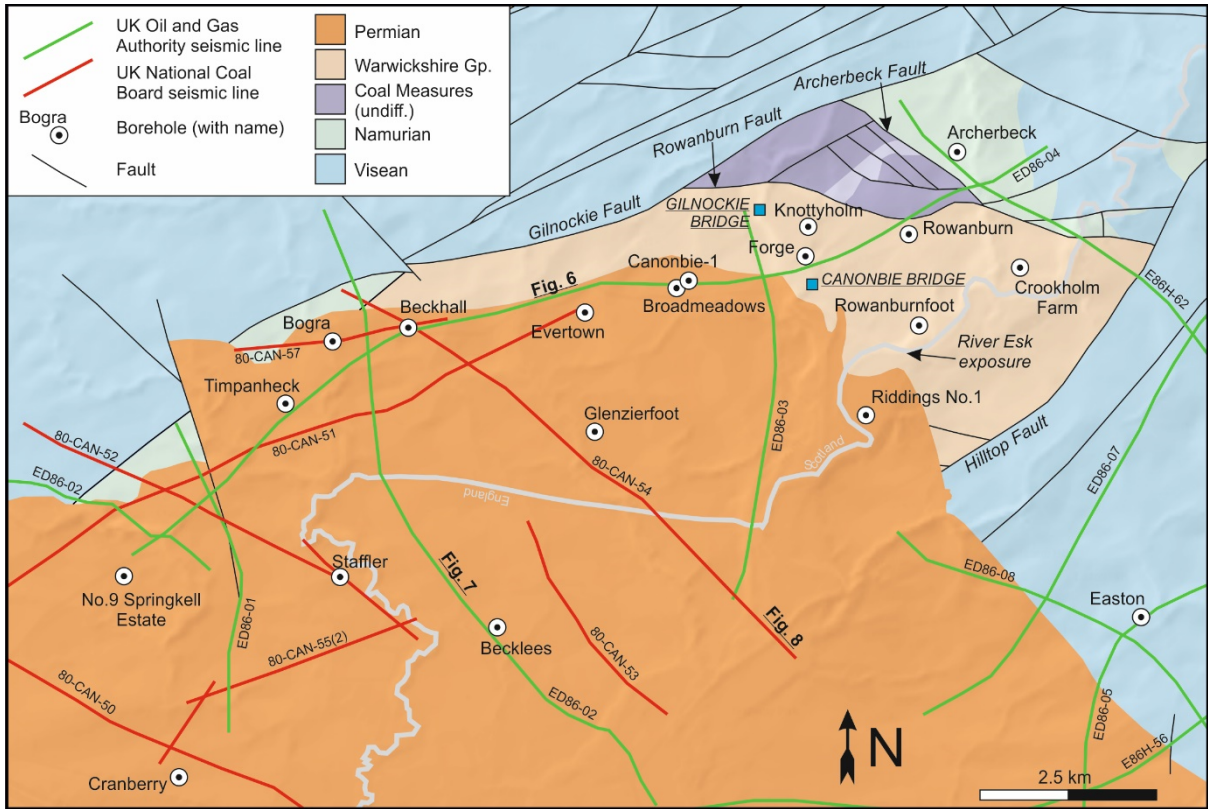
944 Fig. 11a: A plate tectonic setting map for the North Patagonian Andes and the North Patagonian
945 broken foreland (based on Gianni et al., 2015). A Stephanian-Autunian palaeogeographic
946 reconstruction of the Variscan foreland basin system of the British Isles based partly on Peace and
947 Besly (1997) and the findings of this study. 11c: A schematic cross-section of the North Patagonian
948 Andes, the North Patagonian fold and thrust belt (FTB), North Patagonian foredeep and the North
949 Patagonian broken foreland (from Bilmes *et al.*, 2013). 11d: A schematic late Westphalian
950 reconstruction of the Variscan collision zone, external Variscides, Variscan foredeep and the northern
951 British broken foreland. LDB = Lake District Block; ISZ = Iapetus Suture Zone; SSU = Scottish Southern
952 Uplands; MVS = Midland Valley of Scotland.

953



954

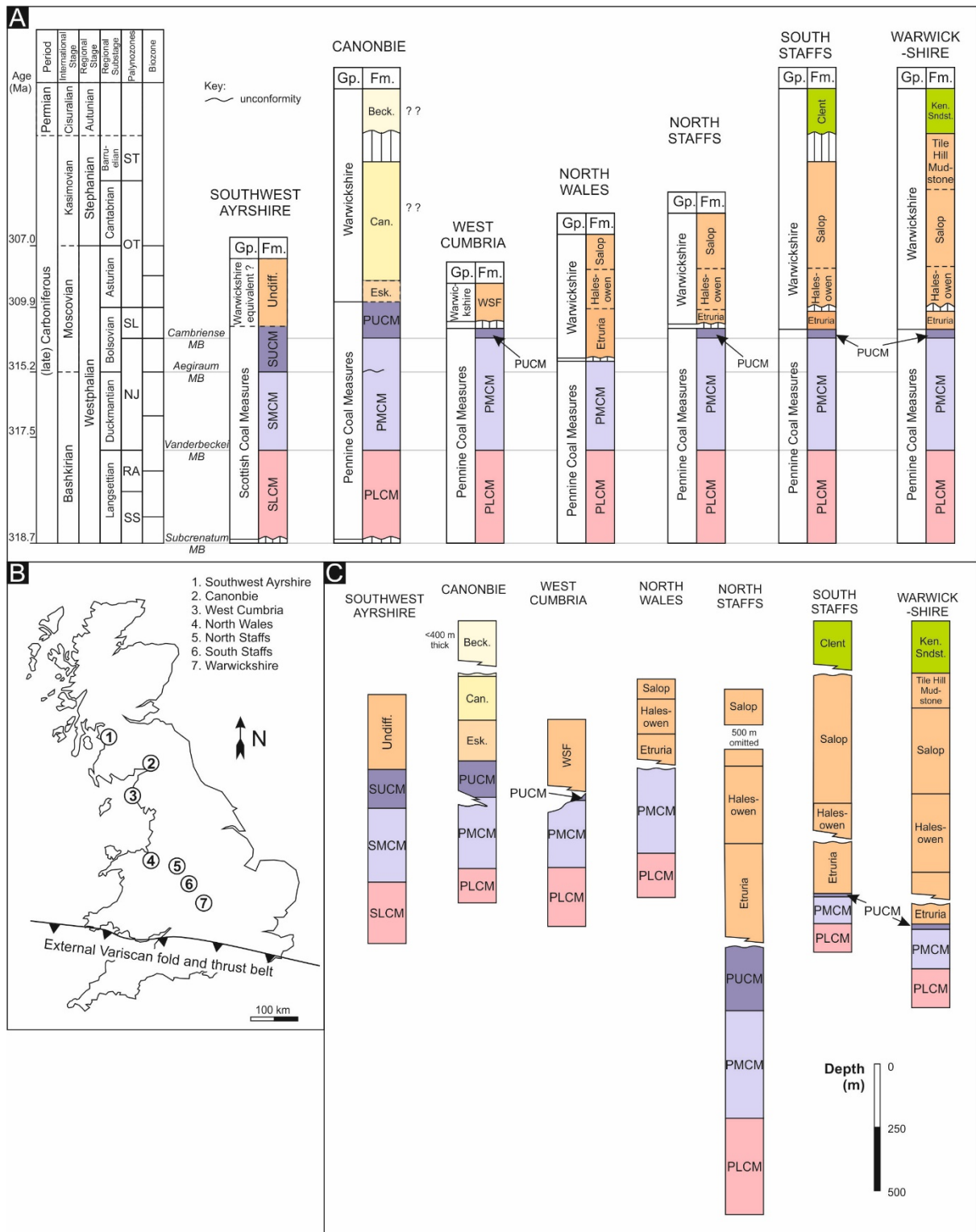
955 Fig.1



957

958 Fig. 2

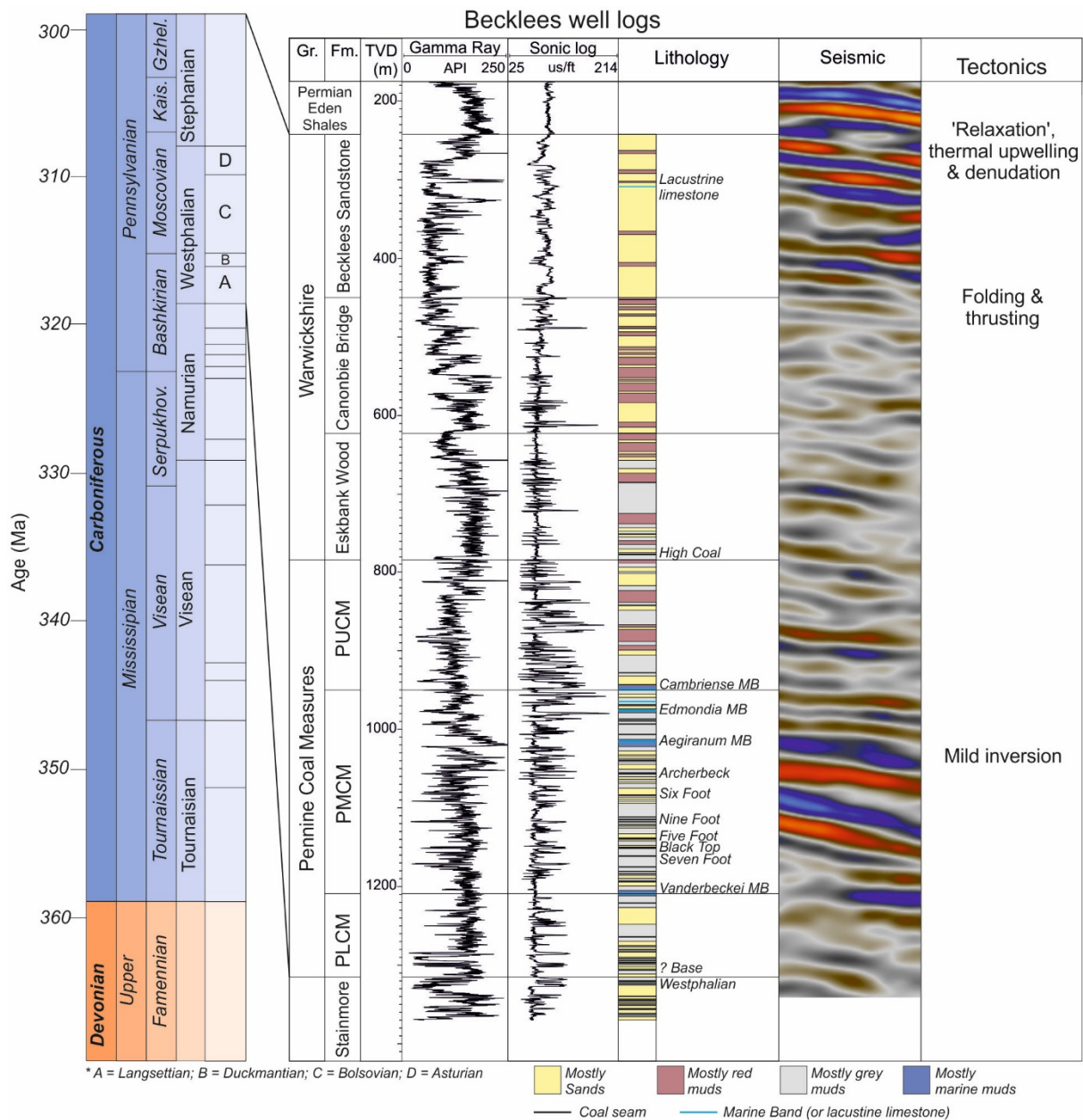
959



960

961 Fig. 3

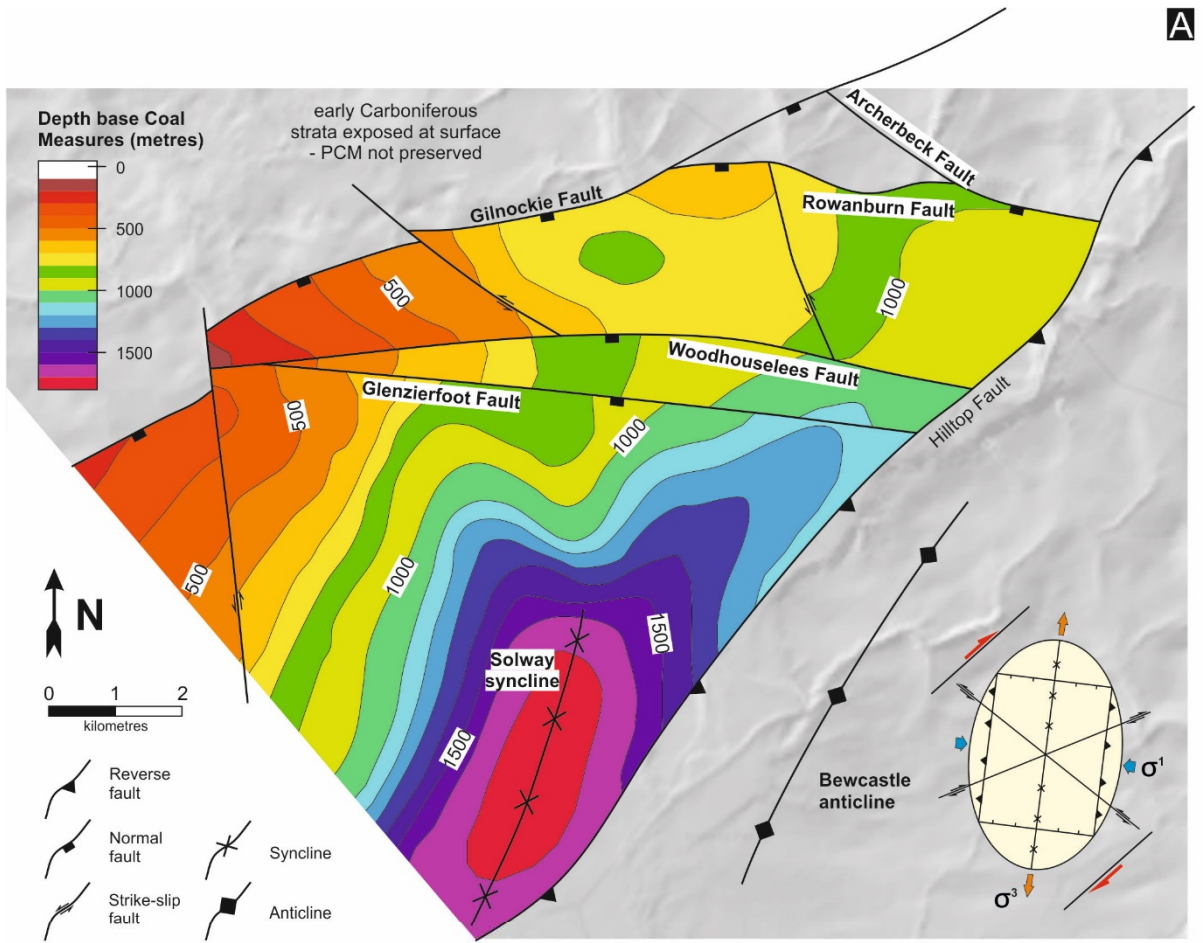
962



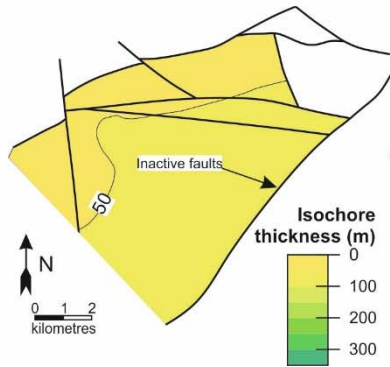
963

964 Fig. 4

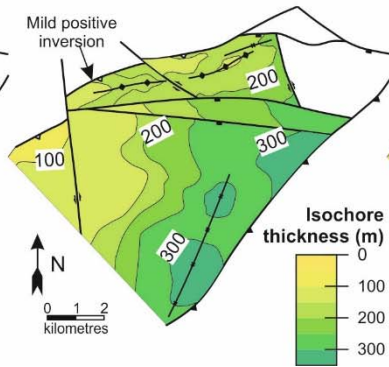
965



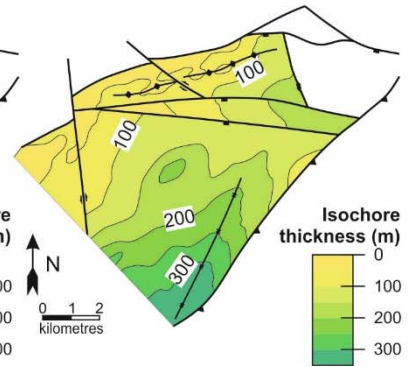
B Pennine Lower Coal Measures



C Pennine Middle Coal Measures



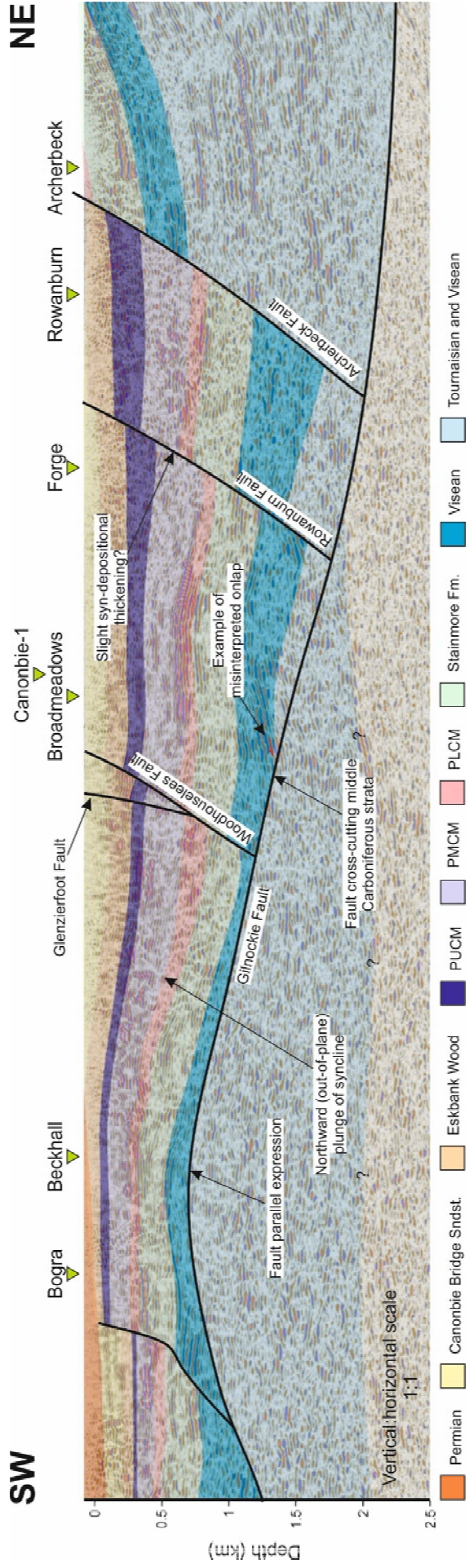
D Pennine Upper Coal Measures



966

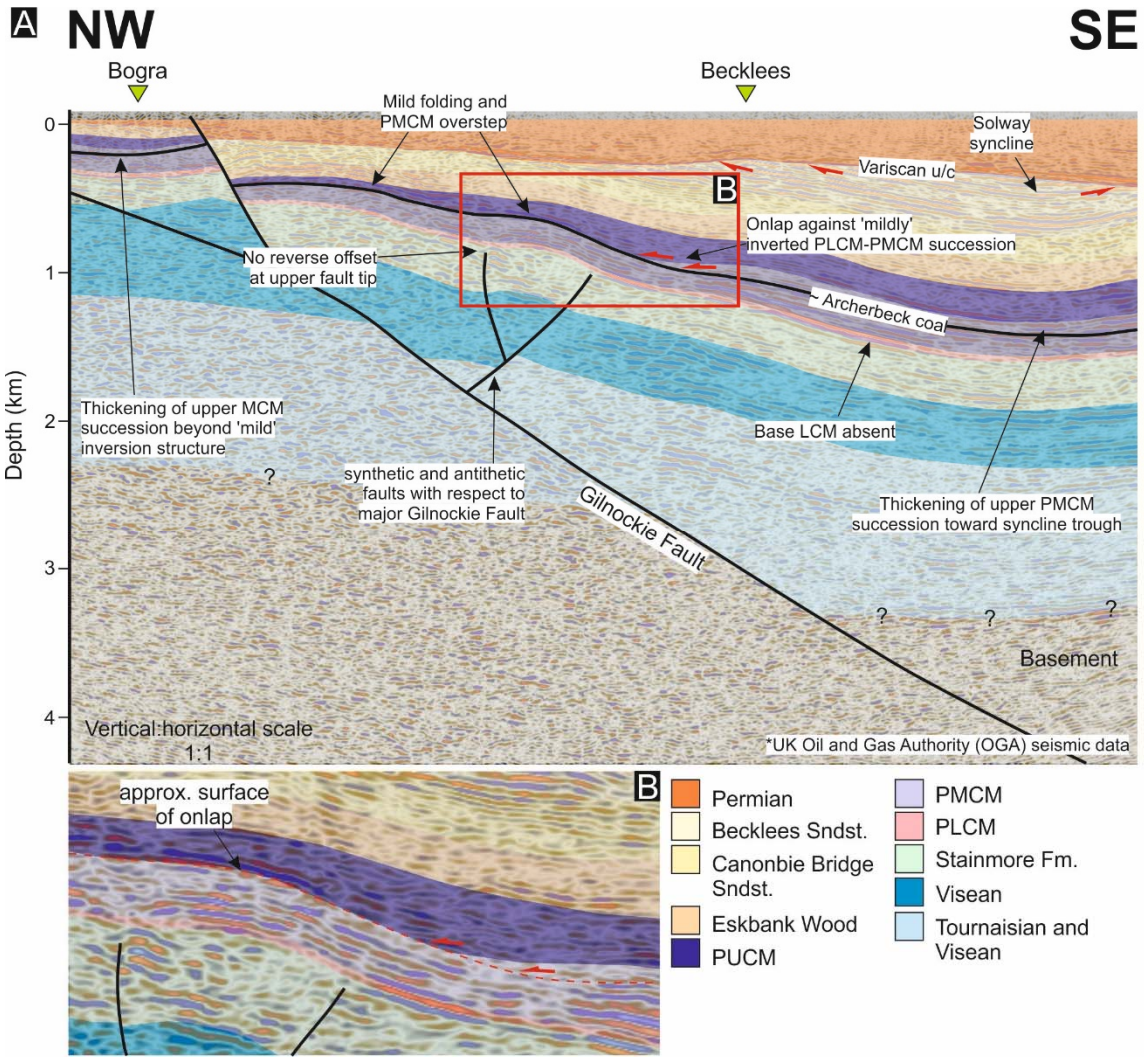
967 Fig. 5

968



970 Fig. 6

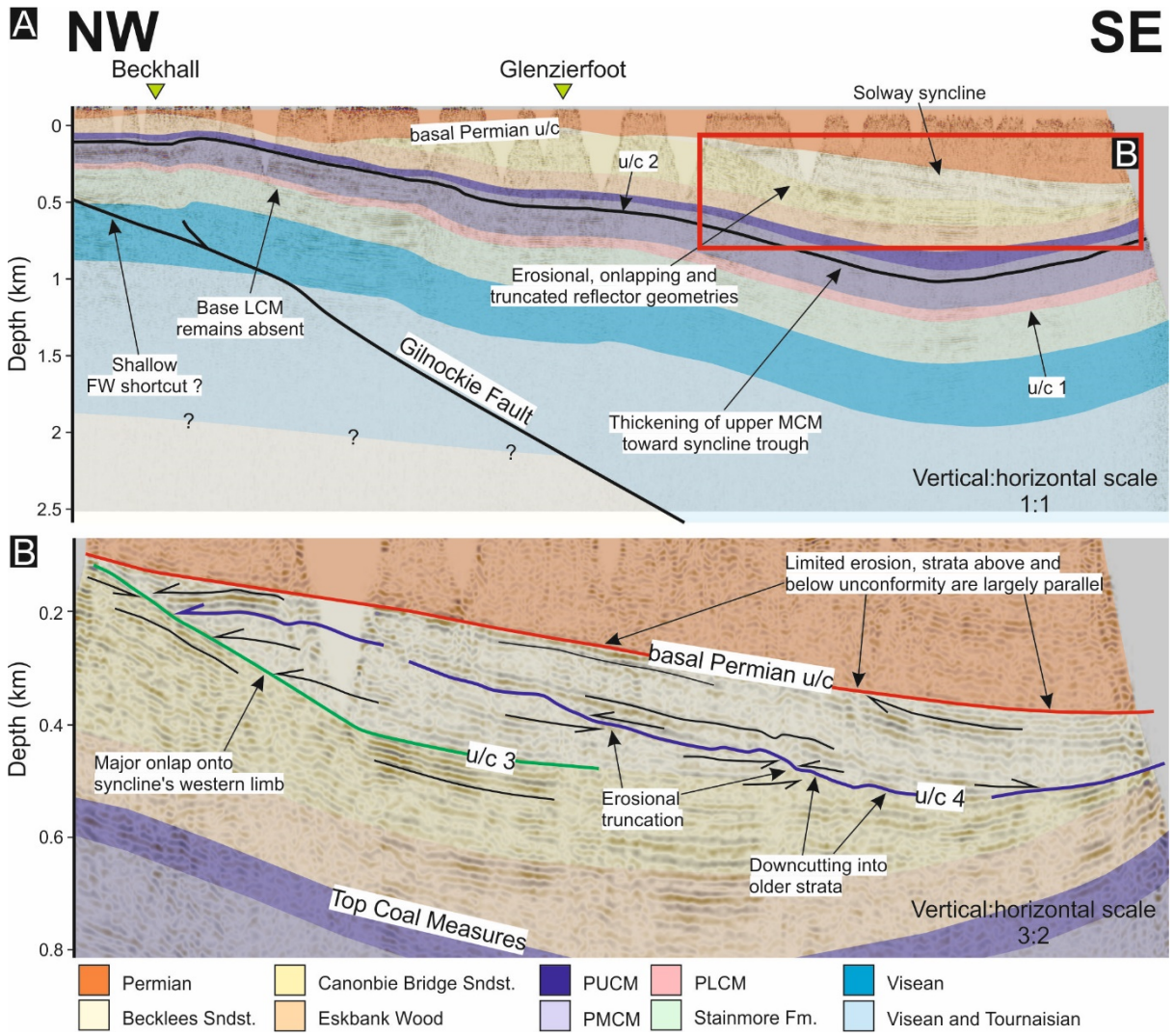
971



975

976 Fig. 8

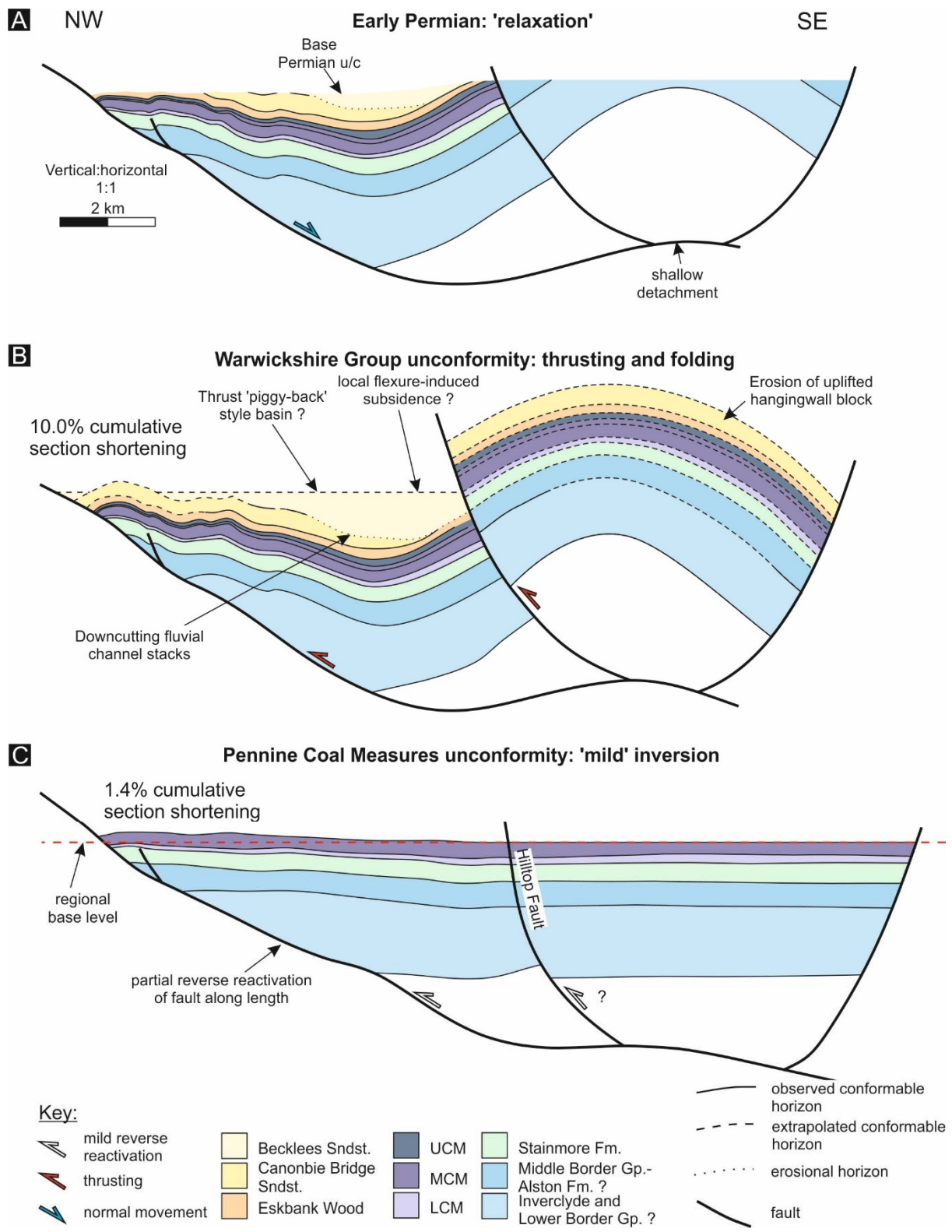
977



978

979 Fig. 9

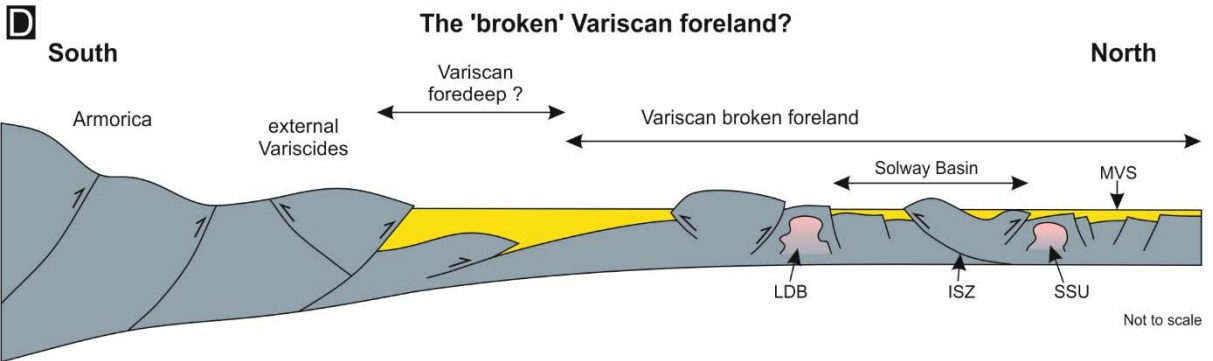
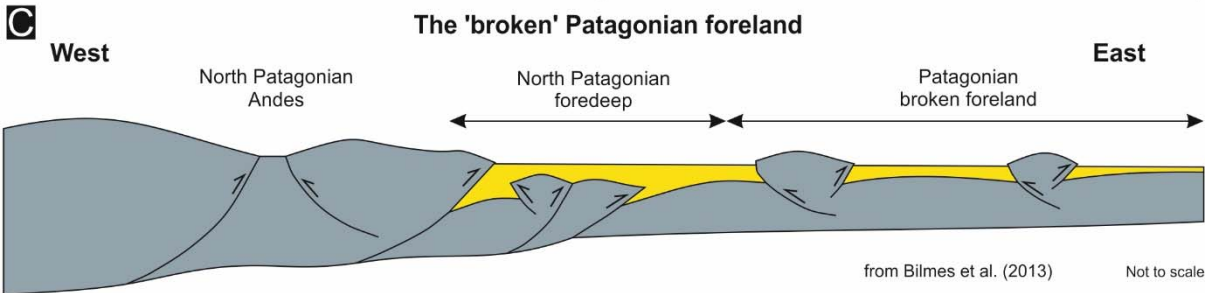
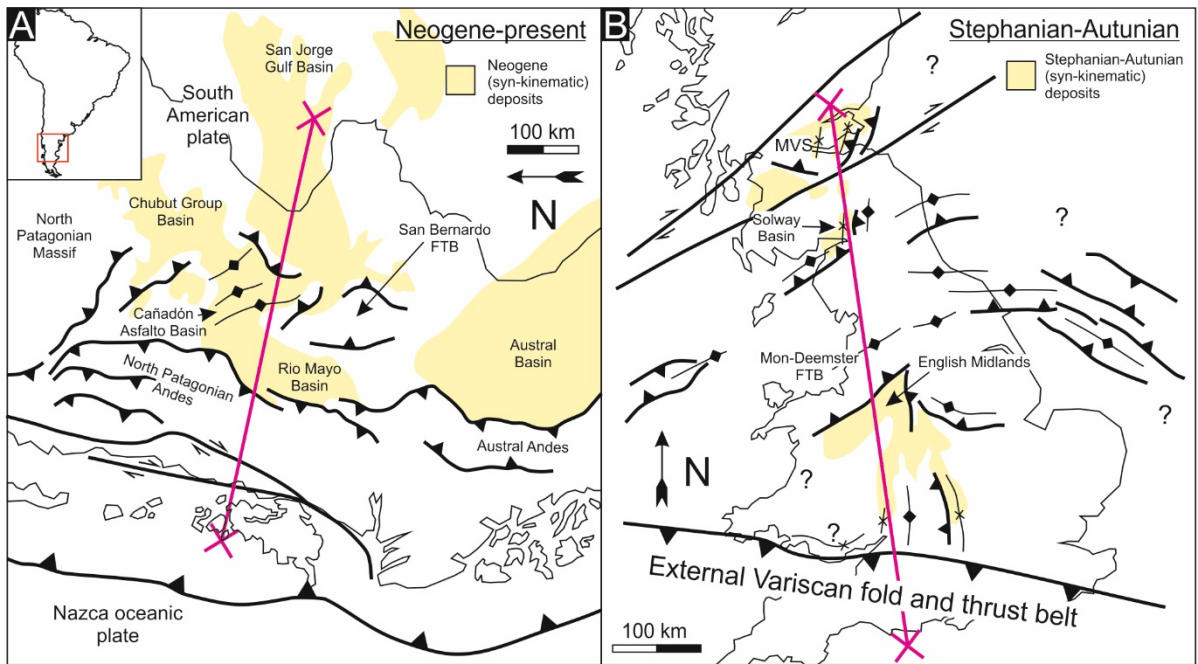
980



981

982 Fig. 10

983



984

985 Fig. 11

986